

JAERI-M

8 8 3 6

FUEL FAILURE BEHAVIOR OF PCI-REMEDY FUELS UNDER
THE REACTIVITY INITIATED ACCIDENT CONDITIONS

May 1980

Tsutao HOSHI, Koji IWATA, Tomio YOSHIMURA^{*}
and Michio ISHIKAWA

この報告書は、日本原子力研究所が JAERI-M レポートとして、不定期に刊行している研究報告書です。入手、複製などのお問い合わせは、日本原子力研究所技術情報部（茨城県那珂郡東海村）あて、お申しこしてください。

JAERI-M reports, issued irregularly, describe the results of research works carried out in JAERI. Inquiries about the availability of reports and their reproduction should be addressed to Division of Technical Information, Japan Atomic Energy Research Institute, Tokai-mura, Naka-gun, Ibaraki-ken, Japan.

Fuel Failure Behavior of PCI-remedy Fuels
under the Reactivity Initiated Accident Conditions

Tsutao HOSHI, Koji IWATA, Tomio YOSHIMURA* and Michio ISHIKAWA

Division of Reactor Safety, Tokai Research Establishment, JAERI

(Received April 4, 1980)

The Zirconium-lined cladding fuel and Copper-barrier fuel developed as PCI-remedy fuels by General Electric Company were tested in the Nuclear Safety Research Reactor (NSRR) to examine the fuel behavior under the reactivity initiated accident (RIA) conditions.

Besides the above two remedy fuels, the currently used BWR type fuel was also tested for reference.

Slightly higher cladding surface temperature was indicated in the Copper-barrier fuel than in the Zirconium-lined and the reference fuel. However, no significant differences were observed between the three in failure threshold and fuel failure behavior.

Keywords; Pellet-Cladding Interaction Remedy Fuel, Zirconium-lined Fuel, Copper-barrier Fuel, Reactivity Initiated Accident, NSRR Reactor, Fuel Failure, Fuel Behavior, Reactor Safety

* Cooperative Research Scientist; Ship Research Institute

反応度事故条件下における PCI 対策改良型燃料の破損挙動

日本原子力研究所東海研究所安全工学部

星 篤雄・岩田 耕司・吉村 富雄*・石川 迪夫

(1980 年 4 月 4 日 受理)

PCI 対策燃料として米国 GE 社で開発されている、ジルコニウム内張り型燃料ならびに銅バリヤ燃料についての反応度事故条件下における挙動を調べるために、NSRR で照射実験を行なった。照射実験では上述 2 種類の燃料棒の他に、比較用としてこれまでの BWR で用いられている在来型燃料棒を照射した。

照射実験の結果、照射中の銅バリヤ燃料の被覆管表面温度は他の 2 者よりも若干高い傾向がみられたが、燃料の破損しきい値ならびに破損挙動には、上述の三種類の燃料に大きな差異は認められなかった。

* 協力研究員：船舶技術研究所

Contents

1. Introduction	1
2. Experimental method	1
2.1 Test facility	1
2.2 Test capsule	1
2.3 Test fuels	1
2.4 Instrumentation	2
3. Test results and discussion	2
3.1 Energy deposition and power distribution	2
3.2 Fuel behavior	3
3.3 Failure threshold	5
3.4 Cladding surface temperature	5
3.5 Deformation of cladding	6
3.6 Mechanical energy release	6
4. Conclusion	8
Acknowledgements	9
Reference	9

Appendices

A. Magnified views of fuel rods at failure portions	33
B. Transient records during irradiation	33
B-1 ~15 Cladding surface temperature	33
B-16~18 Water column velocity and capsule internal pressure	33
B-19~25 Cladding elongation	33
C. Profile measurement of cladding radial deformation	33
D. NSRR standard fuel rod tests	33
D-1 Shema of NSRR standard fuel rod	33
D-2 Appearance of post-test fuel rods in the NSRR standard fuel rod tests related with energy deposition	33

目 次

1. はじめに	1
2. 実験方法	1
2.1 実験設備	1
2.2 実験カプセル	1
2.3 実験燃料	1
2.4 計 装	2
3. 実験結果と考察	2
3.1 発熱量および発熱分布	2
3.2 燃料挙動	3
3.3 破損しきい値	5
3.4 被覆管表面温度	5
3.5 被覆管の変形	6
3.6 機械的エネルギー	6
4. 結 論	8
謝 辞	9
参考文献	9
附 録	33
A. 燃料破損部拡大写真	33
B. 照射中過渡記録	33
B-1~15 被覆管表面温度	33
B-16~18 水塊速度およびカプセル内圧	33
B-19~25 被覆管伸び	33
C. 被覆管の半径方向変形プロファイル	33
D. NSRR 標準燃料試験	33
D-1. NSRR 標準燃料概略図	33
D-2. NSRR 標準燃料試験における試験燃料の照射後外観	33

1. Introduction

Irradiation of GE-type fuel rods in the NSRR (Nuclear Safety Research Reactor) was requested by the U.S. NRC to investigate the fuel behavior of the PCI remedy fuels under the reactivity initiated accidental conditions (RIA) in accordance with the research participation and technical corporation with the U.S. NRC and the JAERI.

Three types of fuel rods, currently used GE-reference type fuel rod, Zr-lined cladding fuel rod and Cu-barrier cladding fuel rod, were supplied by the U.S. NRC to the JAERI and tested in the NSRR. Total of 21 fuel rods were irradiated until October, 1979, with the NSRR standard water capsule as the first stage of tests.

Energy deposition to the fuel rods was in the range of 150 to 400 cal/g·UO₂ and fuel failure behavior and failure threshold were especially investigated. Summary of the test results is presented in this paper.

2. Experimental Method

2.1 Test facility

The NSRR is a modified TRIGA-Annular Core Pulse Reactor having a large experimental cavity in the core. Figs. 1 and 2 show the general arrangement of reactor facility and the cross section of the core.

Pulsing power is realized by quick withdrawal of transient rods and the maximum reactor capabilities in pulse operation are the peak reactor power of 21,000 MW, total energy release of 117 MW-sec with the pulse width of 4.4 msec as shown in Fig. 3. The major characteristics of the NSRR is shown in Table 1.

2.2 Test capsule

In these experiments, the NSRR standard water capsule was used. Fig. 4 shows the capsule in which the test rod is supported at the center. Cooling water is filled up to 22 cm below the top of capsule flange.

2.3 Test fuels

The three types of fuel rods were tested. One is the currently used GE-reference type fuel rod and the others are Zr-lined cladding fuel rods

and Cu-barrier cladding fuel rods which are newly developed as PCI remedies.

Zr-lined cladding fuel rod has a zircaloy cladding with a metallurgically bonded layer zirconium ($\sim 75 \mu\text{m}$) on the inner surface, and Cu-barrier cladding fuel rod has a zircaloy cladding with a very thin layer ($\sim 5 \sim 10 \mu\text{m}$) of copper plated on the inner surface. Schema and design summary of fuel rods tested are given in Fig. 5 and Table 2.

2.4 Instrumentation

Major instrumentations in the capsule are indicated in Fig. 4.

Cladding surface temperatures were measured by very thin bare-wire Pt/Pt-13%Rh thermocouples attached to the cladding surface by spot welding. Pressure pulses in the capsule were measured by strain gauge type pressure transducer at the bottom of the capsule. Upwards velocity of water column was measured by a float type movement sensor, and the transient displacement of fuel rod by LVDT (Linear Variable Differential Transformer).

Characteristics of the sensors are summarized in Table 3 and the location of the cladding surface thermocouples is shown in Fig. 6.

3. Test results and discussion

The tests consist of two categories, i.e. test for evaluation of energy deposition to the fuel rod and test to obtain information about fuel failure behavior and fuel failure threshold. Eight rods for GE-reference type fuel, seven for Zr-lined fuel, and six for Cu-barrier fuel were irradiated.

The test conditions and summary of the results are listed in Tables 4 and 5.

3.1 Energy deposition and power distribution

The energy deposition to the fuel rod was evaluated by the method of absolute measurement of fission products, ^{137}Cs , ^{140}Ba , and Zr in pellets after pulse irradiation. The results are shown in Table 6.

The core release energy in Test No. 501-1 was 49.6 MW-sec, then the radially averaged energy deposition at axial center position to the GE-fuel rod was $4.21 \text{ cal/g} \cdot \text{UO}_2\text{-MW-sec}$.

Axial power distribution measured by r-scanning and radial power

distribution calculated are shown in Figs. 7 and 8, respectively.

3.2 Fuel behavior

The appearance, X-ray photographs and neutron radio-graphs of irradiated fuel rods are shown in Figs. 9, 10 and 11 and magnified view for the typical portion of failed fuel rods are shown in Appendix A.

Reference type fuel (Test series 501): Reference type fuels were tested at energy deposition of 169 cal/g·UO₂ (Test No. 501-2), 209 (501-1), 257 (501-3), 277 (501-10), 284 (501-4), 305 (501-7) and about 390 cal/g·UO (501-8 and 501-9).

In Test No. 501-2, (169 cal/g·UO₂), the cladding was partially oxidized and it is concluded that the DNB condition just occurred.

The fuel rod in Test No. 501-1 (209 cal/g·UO₂) was fully oxidized and, in Test No. 501-3 (257 cal/g·UO₂) and 501-10 (270 cal/g·UO₂) oxide flakes were observed in both rods, but neither of the fuel rods failed.

In Test No. 501-4 (284 cal/g·UO₂), melted cladding / or fuel was pushed out from the cladding at the lower portion of the rod (Appendix A-1). Relatively large ballooning of the cladding was observed at the lower portion of the rod and several holes were at the thermocouple locations.

The fuel rod in Test No. 501-7 (305 cal/g·UO₂) was broken into two pieces by the embrittlement of cladding during disassembling. Some void space was observed in the fuel at the fractured portion (Appendix A-2). In the X-ray photograph and the neutron radiography (Fig. 10(1) and Fig. 11(1), extensive movement of fuel pellets was found

In Test No. 501-8 (393 cal/g·UO₂), the cladding had extensively melted. The fuel rod was fractured into three pieces during disassembling. Melted fuel had adhered to the lower failed portion of the rod, but almost all of the fuel was expelled from the rod as seen in the neutron radiography (Fig. 11(1) and fragmented. Extensive oxidation of cladding at the fuel plenum portion and shortening of the spring were observed (Fig. 10(1) and 11(1).

The transient records of capsule pressure and water level sensor (Appendices B-16, B-17 and B-18) indicate that the fuel failure occurred just after the power burst.

The major difference of fuel behavior in Test No. 501-8 from that of the NSRR standard fuel rod tests under such the high energy deposition

tests is that the fuel meat was expelled and fragmented but the cladding did not fragment.

Fragmentation of fuel and cladding resulted from melting of UO_2 pellets and cladding. However, in case of the GE fuel rod tested, it is supposed that no fragmentation of the cladding might result from that the melted fuel was expelled early from the cladding so that the cladding temperature rise was limited and significant melting of cladding did not occur. Because extensive pressure increased due to the evaporation of UO_2 is expected at the lower end of fuel stack, where is the maximum power peaking position,*1) since the gas plenum of lower portion of the rod is very small compared with that of the NSRR standard type fuel rod as shown in Appendix D-1.

In Test No. 501-1, therefore, a fuel rod wrapped with the cadmium (Cd) sheet at the both ends of fuel stack was irradiated to investigate the effects of pressure generation at the edge of fuel stack. As the results, the fuel and the cladding had fragmented in the same manner as that of the NSRR standard type fuel rod as seen in Appendix D-2.

Zr-lined fuel (Test series 502): Zr-lined fuels were tested at energy depositions of 171 cal/g· UO_2 (Test No. 502-2), 208 (502-1), 287 (502-6), 304 (502-4), 309 (502-4b), 313 (502-3) and 394 (502-5).

The fuel behaviors of Zr-lined rods are almost the same as those of the GE-reference type rods except the fuel rod in Test No. 502-6 fractured into two pieces and the fuel rod in Test No. 502-4 did not fail even though the energy deposition was over 300 cal/g· UO_2 .

Test No. 502-4b was the reproducibility test of Test No. 502-4. The irradiation condition was the same as that of Test No. 502-4, but the fuel rod failed. The state of failure was almost similar manner to that of the reference type fuel rod in Test No. 501-7 which was subjected to the same energy deposition.

*1) Axial and radial power peaking factors are 1.28 and 1.30 (Figs.6 and 7), respectively, and then the energy deposition at the edge of the lowest pellet of fuel stack is 666 cal/g· UO_2 when a radially averaged energy of 400 cal/g· UO_2 is deposited at the axial center.

Cu-barrier fuel (Test series 503): Cu-barrier fuels were tested at energy deposition of 169 cal/g·UO₂ (Test No. 503-2), 201 (503-1), 280 (503-3b), 283 (503-3), 304 (503-4) and 392 (503-5).

The appearances of rods in Test Nos. 503-1 & 2 were almost the same as those of reference rods but, in Test No. 503-3, the rod was broken into two pieces. Test No. 503-3b was the reproduceability test of Test No. 503-3. The fuel failure behavior was almost the same as that of Test No. 503-3 although the rod had not fractured. The fuel rods in Test Nos. 503-4 & 5 failed in a similar manner to the reference type rods.

In general, extent of damage by appearance was rather milder in the GE fuel rods tested than in the NSRR standard fuel rods. This may probably have resulted from the larger cladding thickness which secured higher rigidity of the cladding during RIA transient. In the NSRR test with thinner cladding rods in which cladding thickness was reduced to about 65 % of the standard, failure threshold has decreased by about 50 cal/g·UO₂ and more intensive damage to the rod was observed.

3.3 Failure threshold

Failure thresholds for each type of fuel rod are compared in Fig. 12 with that for the NSRR standard fuel rod.

The failure threshold energy for the reference fuel rod and both the remedy fuel rods is 260 to 280 cal/g·UO₂ which is equal to or a little higher than that for the NSRR standard fuel rod. A single exception is that a Zr-lined rod did not fail at 300 cal/g·UO₂ as described in the preceding section.

3.4 Cladding surface temperature

The maximum cladding surface temperatures at the axial center position are shown in Fig. 13 with the data for NSRR standard fuel rods. Transient records are attached in Appendices B-1 to B-15.

The cladding surface temperatures at an energy deposition of 170 cal/g·UO₂ indicate DNB condition occurred in each case.

The maximum cladding surface temperatures in case of the Cu-barrier fuel rods are higher than those in the GE-reference fuel and the Zr-lined fuel rods at lower energy depositions. It is considered that these differences may be the result of the good heat conductivity in the fuel-cladding gap due to melting of Cu-barrier and it is reasonable that this

effect disappeared at high energy depositions, because the zircaloy base reached melting temperature promptly at the energy of near failure threshold.

3.5 Deformation of cladding

Cladding radial deformation

Permanent radial deformation of cladding was measured by the profile meter and measured data are attached in Appendix C.

Fig. 14 shows the maximum and average deformation at the axial center of fuel rod. Permanent deformation increases with increasing energy deposition and is supposed to be caused by the thermal expansion of the fuel pellet since the deformation measured agrees with the value calculated by the thermal expansion of fuel pellet.

However, as seen in the figures of Appendices C-3 & C-5, the large ballooning of cladding is observed in Test Nos. 501-4 & 502-4 of which energy deposition is 280 to 300 cal/g·UO₂. As discussed in the preceeding section 4.2, the energy deposition at the edge of fuel stack might exceed 450 cal/g·UO₂. Therefore, the ballooning seems to be the result of increasing of the fuel rod internal pressure due to evaporation/or melting of fuel pellets at the edge of fuel stack.

Cladding axial deformation

In several tests, measurements of the cladding axial deformation, i.e. elongation, were made with the linear variable differential transformer (LVDT). Transient records are attached in Appendices B-19 to B-25 and the maximum elongation for each tests is compared in Fig. 15 with the data of the NSRR standard fuel rod tests.

Time historical response of the cladding elongation responds to that of the cladding temperature and the maximum value of elongation agrees well with the thermal expansion of cladding evaluated by the maximum cladding surface temperature, therefore, it is concluded that the elongation of cladding depends strongly on the cladding temperature behavior.

3.6 Mechanical energy release

Capsule internal pressure and upward velocity of water column were measured in the tests of 501-8, 502-5 and 503-5 where the energy deposition was about 400 cal/g·UO₂.

Generation of capsule pressure and jump-up of water column were recorded just after the power burst as seen in Appendix A. Maximum value of capsule pressure is 1.5 to 3.4 bar and maximum value of water column velocity is 2.8 to 5.5 m/sec. Those values are almost the same as those of the NSRR standard fuel rod tests at the same energy deposition as shown in Fig. 16.

If it is assumed that the water column moves upward essentially as a solid body, the mechanical energy generated by the fuel failure can be evaluated by adding the two components, i.e. the kinetic energy of the water column and the energy imparted to the air contained in the top part of the capsule by compression since the potential energy of water column and the strain energy contained within the capsule wall are negligible.

The kinetic energy of the capsule water column is calculated by the equation

$$E_k = \frac{1}{2} m u^2 \quad (1)$$

where

E_k ; Kinetic energy of water column

m ; mass of upward moving water column

u ; velocity of water column

The energy imparted to the air by compression is given by the equation, if the air is compressed adiabatically,

$$\begin{aligned} E_c &= \int_{V_o}^V p dv \\ &= \frac{1}{\gamma-1} (P_o V_o - P V) \end{aligned} \quad (2)$$

where

E_c ; energy imparted to the air

P_o ; initial pressure of air (1 atm)

V_o ; initial volume of air space in the top part of the capsule
(2486 cm³)

P ; air pressure at time when the air compressed to volume V

V ; volume of the air compressed by the upward movement of the water column.

γ ; C_p/C_v of air (1.4)

In the equation (2), P and V are given by the equations

$$P = P_0 \left(\frac{V_0}{V} \right)^\gamma \quad (3)$$

$$V = A (L_0 - h) \quad (4)$$

where

A ; cross-sectional area of the capsule (113 cm²)

L₀ ; initial height of air space (22 cm)

h ; upward displacement of water column

Assuming that the water above the top of the fuel moves as a solid body, the mass of water column is 2.26 kg (the height of the water column is about 20 cm) and, then, the mechanical energy generated by the fuel failure is calculated from the data of the velocity and the height of water column recorded by the velocity transducer. The energy conversion ratio defined by the following equation is then obtained.

$$\eta = \frac{E_m}{E_n} \quad (5)$$

where

η ; the energy conversion ratio

E_m ; amount of mechanical energy (E_k + E_c)

E_n ; fission energy in the fuel up to time when E_m is evaluated.

The mechanical energy and conversion ratio, which are evaluated at the time of peak water column velocity and of maximum water level, are summarized in Table 7.

4. Conclusions

Three types of GE fuel rods, currently used reference fuel rods, Zr-lined cladding fuel rods and Cu-barrier cladding fuel rods, were tested in the NSRR. A total of 21 tests at room temperature and atmospheric pressure have been completed so far.

The experimental results are summarized as follows;

- (1) Failure threshold energy of GE-reference fuel rod is 260 to 280 cal/g·UO₂ which is equal to or a littler higher than that of NSRR standard rods.

- (2) Zirconium-lining had no influences on thermal behavior, nor failure threshold energy.
- (3) Copper-barrier caused higher cladding temperatures at lower energy depositions, but had no evident influences on failure threshold.
- (4) In the view point of fuel failure behavior at the RIA conditions, no significant differences between GE-reference fuel rod and newly developed Zr-lined and Cu-barrier fuel rods are observed.

Acknowledgements

This test program was performed under the research participation and technical cooperation between the U.S. NRC and JAERI. The authors wish to thank Drs. M. Nozawa in JAERI, W.V. Johnstone in U.S. NRC, J. Crocker in Idaho National Engineering Laboratories, and J.S. Armijo in General Electric Co., for their contribution to the promotion of the program.

Authors also thank Dr. E. Coutright in Pacific North West Laboratories and Messrs. T. Fujishiro and S. Kobayashi in JAERI for fuel fabrication and shipment and staff of Reactivity Accident Laboratory and NSRR operation section in JAERI for performing the experiment.

References

- * (1) NSRR Operation Section and Reactivity Accident Lab.; "Start-up tests of NSRR", JAERI-M 6791 (1976)
- (2) S. Saito, et al.; "Measurement and Evaluation on Pulsing Characteristics and Experimental Capability of NSRR", J. Nucl. Sci. and Technol. 14, 226 (1977)
- * (3) T. Ise and Y. Nakahara; "Heat Deposition in a Single Test Fuel Pin in the NSRR", JAERI-M 5613 (1974)
- (4) M. Ishikawa; "First Progress Report of the Nuclear Safety Research Reactor Experiments", 4th LWR Safety Information Meeting, Washington (1976)
- * (5) T. Hoshi, et al.; "Fuel Failure Behavior of Unirradiated Fuel Rods under Reactivity Initiated Conditions", J. At. Energy Soc. Japan, 20, 651 (1978)

* are written in Japanese.

Table 1 Major characteristics of NSRR

<u>Reactor Type;</u>	Modified TRIGA-ACPR (Annular Core Pulse Reactor)
<u>Reactor Vessel;</u>	3.6 ^m (wide) × 4.5 ^m (long) × 9 ^m (deep) open pool
<u>Fuel;</u>	
Fuel type	12 wt% U-ZrH fuel
Fuel enrichment	20 wt% U-235
Clad material	Stainless steel
Fuel diameter	3.56 cm
Clad diameter	3.76 cm O.D.
Length of fuel section	38 cm
Number of fuel rods	157
Equivalent core diameter	62 cm
<u>Control Rods;</u>	
Number	8 (including 2 safety rods)
Type	Fuel followered type
Poison material	Natural B ₄ C
Rod drive	Rack and pinion drive
<u>Transient Rods;</u>	
Number	2 fast transient rods and 1 adjustable transient rod
Type	Air followered type
Poison material	92% enriched B ₄ C
Rod drive	Fast : Pneumatic Adjustable: Rack and pinion & pneumatic
<u>Core Performance;</u>	
a) Steady state operation	
Steady state power	300 kW
b) Pulse operation	
Max. peak power	21,100 MW
Max. burst energy	117 MW-sec
Max. reactivity insertion	3.43% Δk (\$4.67)
Min. period	1.12 msec
Pulse width	4.4 msec (1/2 peak power)
Neutron life time	30 μsec
<u>Experiment Tube;</u>	
Inside diameter	22 cm

Table 2 Characteristics of GE fuel rods

Type of fuel rods tested	
GE reference type fuel rod (8x8 BWR type)	
Zirconium lined fuel rod (Zr- lined)	
Copper barrier fuel rod (Cu- barrier)	
Cladding material	Zr-2
Fuel pellets	
Enrichment	10% U-235
Density	95% T.D.
Geometry	
Dimension	
Pellet O.D.	10.57 mm
Cladding O.D.	12.52 mm
Cladding wall thickness	0.86 mm
Gap width	0.115 mm
Zr-liner thickness	~10 % of wall thickness
Cu-barrier thickness	~0.01 mm

Table 3 Sensors for transient measurement

Measuring Item	Sensor Type	Measuring Range	Response Frequency	Remarks
Cladding Surface Temperature	Pt-Pt.13%Rh T/C Wire Diameter 0.2 mmφ	Room Temp. ~1700°C	~200 Hz	Spot welded to the Cladding Surface
Fuel Internal Pressure	Flash Diaphragm Type Strain Gauge Transducer	0 ~ 500 kg/cm ²	resonance freq. 170 kHz	
Capsule Internal Pressure	"	0 ~ 200 kg/cm ²	responce freq. 110 kHz	
Water Velocity	Float Type Transducer	0.1 ~ 20 m/s		
Fuel Axial Displacement	LVDT	~ ±10 mm	~1 kHz	
Cladding Axial Displacement	LVDT	~ ±10 mm	~1 kHz	

Table 4 Summary of Irradiation Condition on GE Fuel Tests

Type of fuel rod	Test No.	Fuel No.	Date of Irradiation	Pulse No.	Inserted Reactivity	Reactor Period msec	Core Energy Release MW-s	Estimated Energy Deposition cal/g·UO ₂
GE std.	501-1	G 2	11/15/'78	767	2.58	2.63	49.6	209
	2	G 3	1/23/'79	802	2.28	3.25	40.2	169
	3	G 4	1/30/'79	806	3.18	1.90	61.0	257
	4	6	3/15/'79	816	3.31	1.80	67.4	284
	7	G 5	1/31/'79	807	3.55	1.63	72.5	305
	8	G 7	4/ 6/'79	821	4.23	1.28	93.3	393
	9	G 8*1	5/24/'79	849	4.23	1.28	93.6	394
	10	G11*1	8/30/'79	884	3.35	1.77	65.9	277
	502-1	G30	1/24/'79	804	2.58	2.63	49.3	208
	2	G34	3/15/'79	817	2.28	3.25	40.6	171
Zr-lined	3	G36	4/ 5/'79	819	3.58	1.61	74.4	313
	4	G33	2/ 8/'79	808	3.55	1.63	72.3	304
	4b	G46	10/19/'79	909	3.55	1.63	73.3	304
	5	G37	4/ 6/'79	822	4.23	1.28	93.6	394
	6	G45	8/30/'79	885	3.31	1.80	68.2	287
	503-1	G19	1/24/'79	805	2.58	2.63	47.7	201
Cu-barrier	2	G22	3/16/'79	818	2.28	3.25	40.2	169
	3	G24	4/12/'79	823	3.31	1.80	67.2	283
	3b	G26	10/25/'79	910	3.31	1.80	66.5	280
	4	G21	2/ 8/'79	809	3.55	1.63	72.1	304
	5	G25	4/12/'79	824	4.23	1.28	93.1	392

*1 Fuel rod covered with Cd sheet at both ends of fuel stack to reduce power peaking at the edge of fuel stack.

Table 5(a) Summary of test results on GE-reference type fuel rod

Energy deposition (cal/g.UO ₂)	Test No.	Max. cladding surface temperature						Max. capsule pressure (bar)	Max. water column velocity (m/sec)	Max. elongation (mm)	Post-test observation
		#1 (°C)	#2 (°C)	#3 (°C)	#4 (°C)	#5 (°C)	#6 (°C)				
169	501-2	720	700	380	540	600	450	-	-	0.7	Cladding surface was slightly discolored at the fuel region.
209	501-1	1120	1150	1120	1180	1120	1130	-	-	-	Cladding surface was discolored in black over the entire fuel region. Fuel rod did not fail.
257	501-3	1420	1410	1350	1400	1420	1330	-	-	-	Cladding surface was discolored over the entire fuel region and oxidized zircaloy film flaked away. Fuel rod did not fail.
277	501-10	1420	1510	1510	1510	1750	failed	-	-	-	Cladding surface was discolored over the entire fuel region and oxidized zircaloy film flaked away. Fuel rod did not fail.
284	501-4	1690	>1520	1530	1630	1520	1530	-	-	2.9	Melted cladding/or fuel was pushed out from the cladding and relatively large ballooning of cladding was observed at the lower portion of the rod. Several holes were at the thermo-couple locations.
305	501-7	1620	>1670	1600	1640	1640	1620	-	-	3.4	Fuel rod fractured into two pieces during disassembling. Large void in the fuel was observed at the lower fractured portion.
393	501-8	>1150	>1030	>1120	>1120	-	-	2.5	2.8	-	Cladding was melted extensively at the lower portion of rod. Fuel was expelled from the rod and fragmented. Oxidation of cladding was observed at the portion of fuel plenum.
394	501-9	>1620	>1620	>1640	>1580	-	-	~ 0	~ 0	-	Fuel rod was fragmented except the portion where Cd sheet was attached.

Table 5(b) Summary of test results on GE-Zr lined type fuel rod

Energy deposition (cal/g.UO ₂)	Test No.	Max. cladding surface temperature						Max. capsule pressure (bar)	Max. water column velocity (m/sec)	Max. elongation (mm)	Post-test observation
		#1 (°C)	#2 (°C)	#3 (°C)	#4 (°C)	#5 (°C)	#6 (°C)				
171	502-2	640	700	480	710	810	800	-	-	-	Cladding surface was slightly discolored over the fuel region.
208	502-1	1110	1130	1130	1110	1250	1140	-	-	1.5	Cladding surface was discolored in black over the entire fuel region. Fuel rod did not fail.
287	502-6	>1390	1620	>1390	1680	failed	1690	-	-	-	Fuel rod fractured into two pieces.
304	502-4	1510	1500	1480	1500	1410	1510	-	-	-	Cladding surface was discolored and dulled over the entire fuel region. Fuel rod did not fail.
309	502-4b	1700	>1680	1630	>1670	failed	>1670	-	-	-	Fuel rod fractured into two pieces. Void was observed in the fuel and cladding.
313	502-3	1690	1530	1510	1650	1600	1650	-	-	3.6	Fuel rod fractured into two pieces during disassembling. Void was observed in the fuel and melted cladding.
394	502-5	1130	1100	1480	1170	-	-	3.4	5.5	-	Cladding was melted extensively. Fuel was expelled from the rod and fragmented. Oxidation of cladding was observed at the portion of fuel plenum.

Table 5(c) Summary of test results on GE-Cu barrier type fuel rod

Energy deposition (cal/g.UO ₂)	Test No.	Max. cladding surface temperature						Max. capsule pressure (bar)	Max. water column velocity (m/sec)	Max. elongation (mm)	Post-test observation
		#1 (°C)	#2 (°C)	#3 (°C)	#4 (°C)	#5 (°C)	#6 (°C)				
169	503-2	710	730	970	950	830	890	-	-	-	Cladding surface was discolored over the entire fuel region.
201	503-1	1370	1280	1200	failed	1350	1350	-	-	1.7	Cladding surface was discolored in black over the entire fuel region. Fuel rod did not fail.
280	503-3b	950	970	810	950	-	-	-	-	2.8	Fuel rod failed with circumferential cracks.
283	503-3	1090	1610	1580	1410	1640	failed	-	-	2.6	Fuel rod fractured into two pieces during disassembling. Void was observed in the melted cladding at the broken portion.
304	503-4	1500	1550	1430	1590	1580	1620	-	-	-	Fuel rod fractured into two pieces. Large void was observed in the fuel and melted cladding.
392	503-5	1670	1100	1520	1540	-	-	1.5	4.0	-	Cladding was melted extensively. Fuel was expelled from the rod and fragmented. Oxidation of cladding was observed at the portion of fuel plenum.

Table 6 Results of Burn-up Measurement on GE Fuel

- 1) Test No. (Fuel No.) ; 501-1 (G2)
 2) Reactor burst power ; 49.6 MW-sec
 3) Fuel pellets measured ; see Fig. 1
 4) Results of measurement ;

Location	Nuclide measured			Ave.	Energy deposition
	^{137}Cs	^{140}Ba	^{95}Zr		
	$(\times 10^{13} \text{ fissions/g} \cdot \text{UO}_2)$				$(\text{cal/g} \cdot \text{UO}_2)$
1	3.13	3.16	3.15	3.15	208
2	3.18	3.16	3.17	3.17	209
3	3.09	3.11	3.09	3.10	204

Table 7 Mechanical energy and thermal-to-mechanical energy conversion ratio in the high energy deposition tests

Test No.	Type of fuel rod	Energy deposition to fuel		Max. wtr. column velocity (level)	Max. wtr. column level	Mechanical energy calculated from		Thermal-to-mechanical energy conversion ratio
		Until failure	Until max. wtr. level			max. velocity	max. level	
		cal/g·UO ₂		m/sec (m)	m	N-m	(cal)	%
501-8	Reference	393	366	2.8(0.055)	0.08	91(22)	120(29)	0.05 - 0.06
502-5	Zr-lined	394	366	5.5(0.062)	0.125	159(38)	240(57)	0.08 - 0.13
503-5	Cu-barrier	392	366	4.0(0.040)	0.07	90(22)	100(24)	0.05 - 0.06

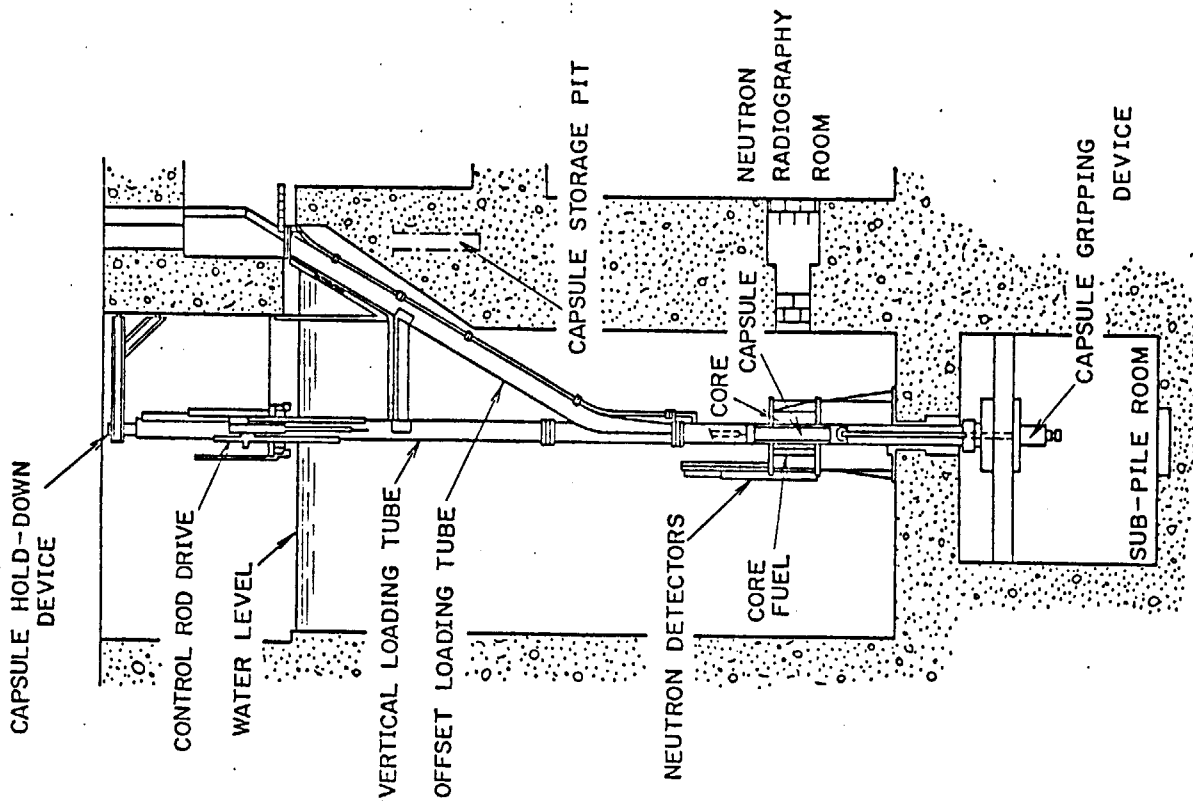


Fig. 1 Vertical cross-section of the NSRR reactor

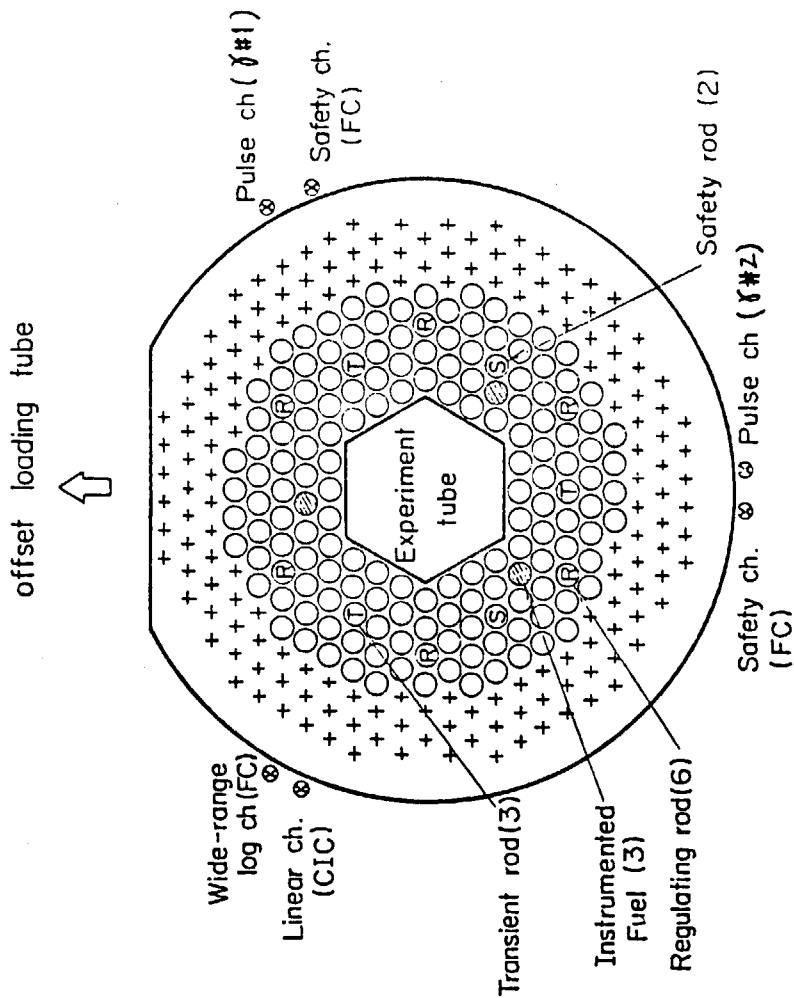


Fig. 2 Standard operating core configuration

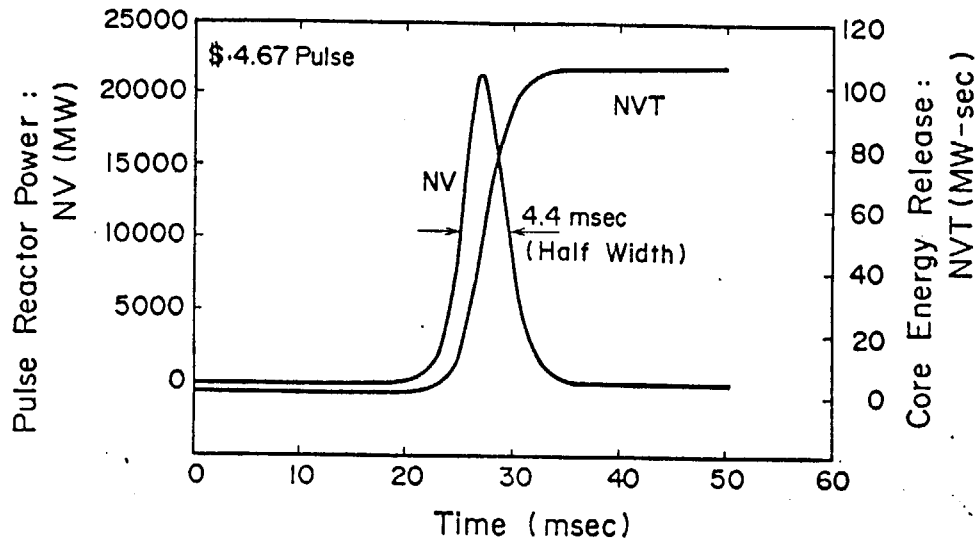


Fig. 3 Histories of reactor power and core energy release in case of maximum reactivity insertion

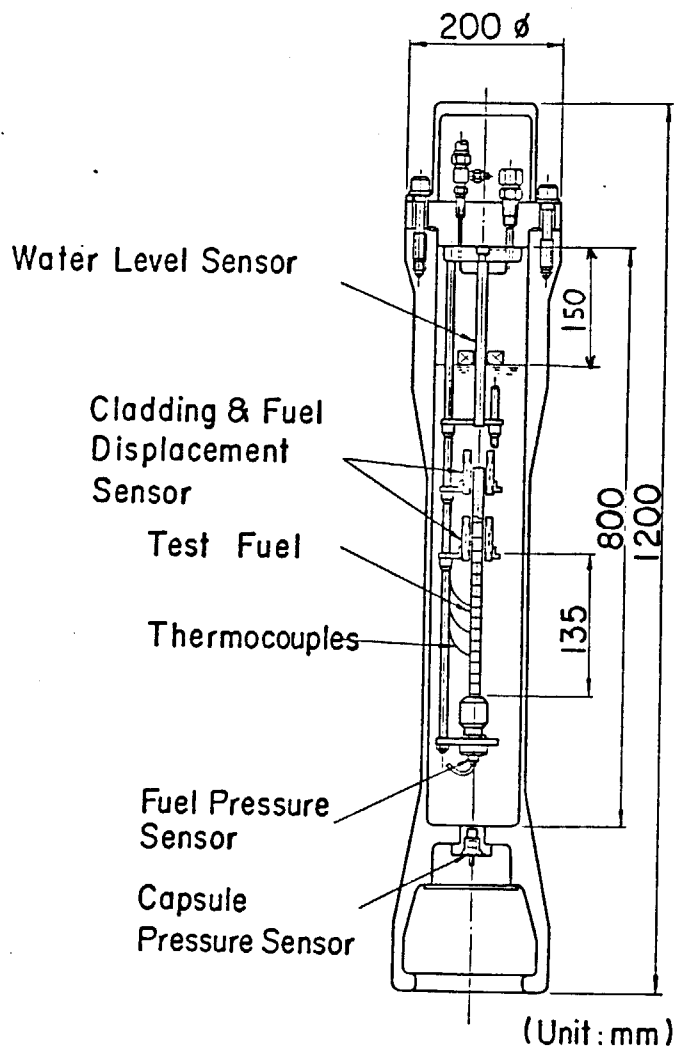


Fig. 4 Standard water capsule

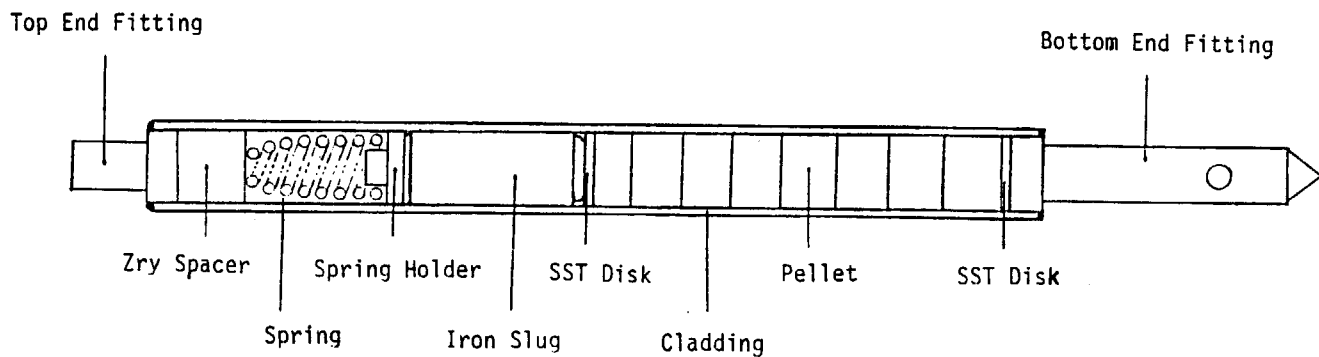


Fig. 5 GE fuel element

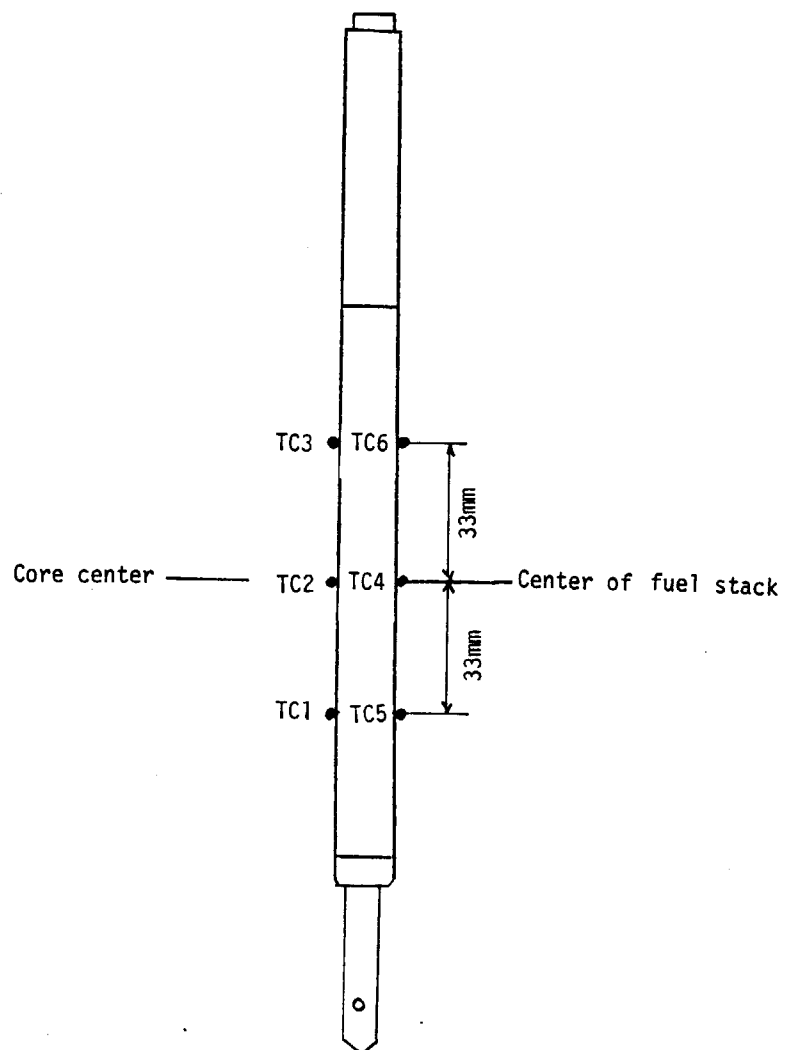


Fig. 6 Location of thermocouples for cladding surface temperature

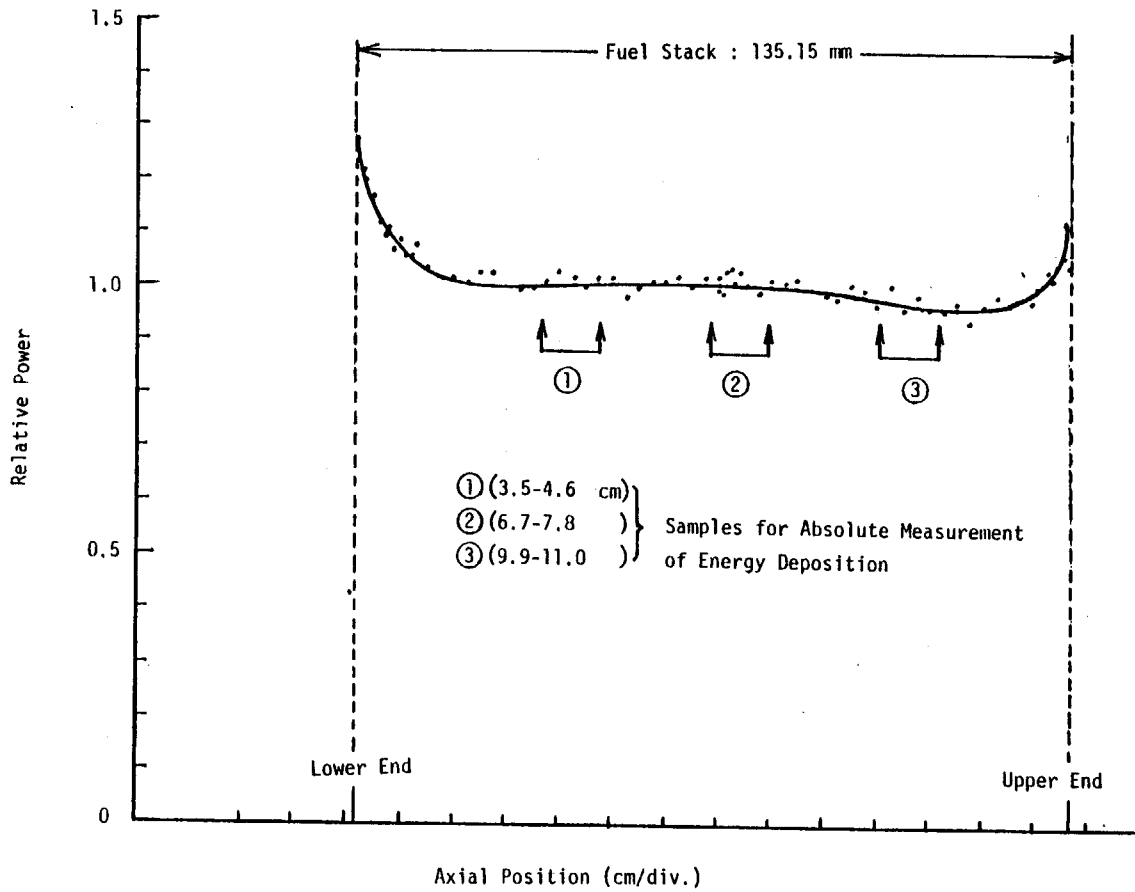


Fig. 7 Axial power distribution : Test No. 501-1

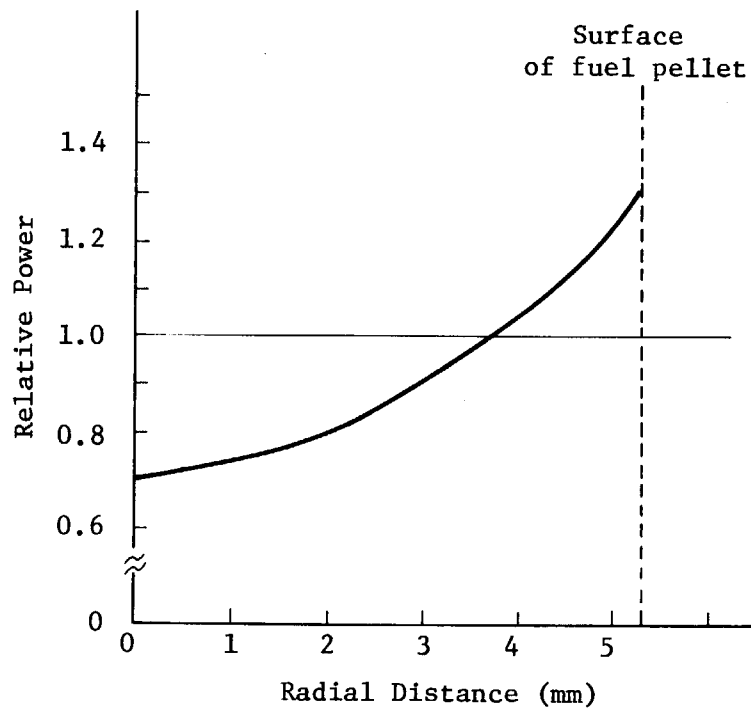


Fig. 8 Pellet radial power distribution (JAERI-M5613)

<u>Test No.</u>	<u>Energy Deposition (cal/g.UO₂)</u>
501-2	169
501-1	209
501-3	257
501-10	277
501-4	284
501-7	305
501-8	393
501-9	394

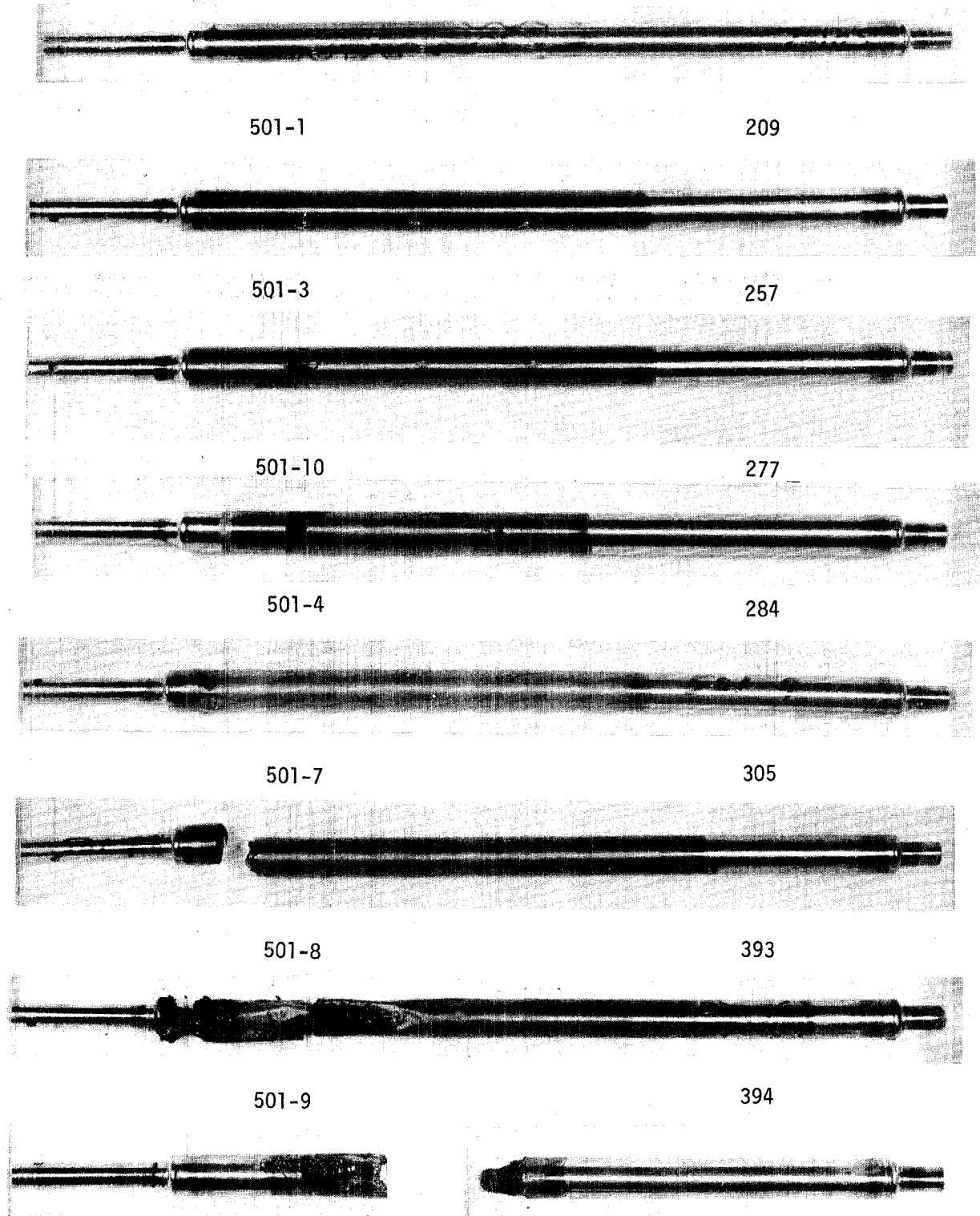
The figure consists of eight horizontal photographs of fuel rods, each corresponding to a row in the table above. The rods are dark, cylindrical, and have various components at their ends, including what appear to be electrical connectors or cladding. The rods are arranged vertically, one above the other, with some showing signs of wear or damage at the ends.

Fig. 9 (1) Post-test photographs of Reference fuel rods

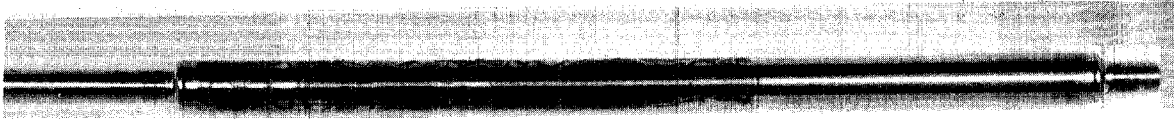


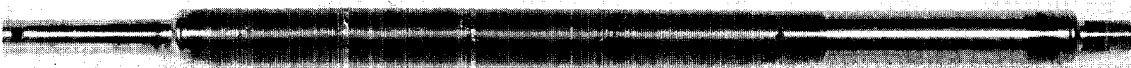
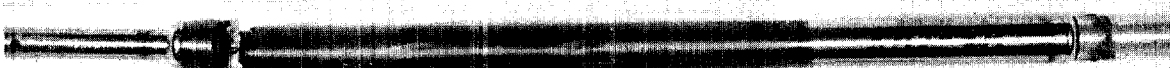
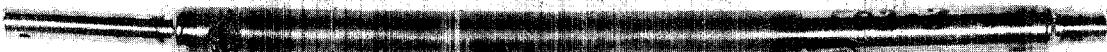
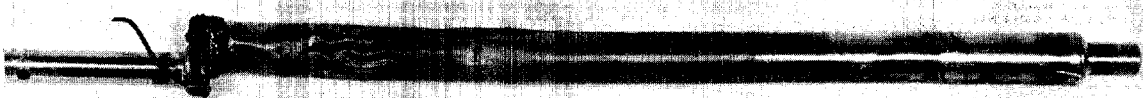
<u>Test No.</u>	<u>Energy Deposition (cal/g.UO₂)</u>
502-2	171
	
502-1	208
	
502-6	287
	
502-4	304
	
502-4b	309
	
502-3	313
	
502-5	394
	

Fig. 9 (2) Post-test photographs of Zr-lined fuel rods

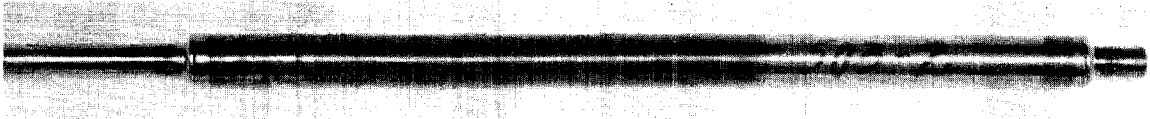
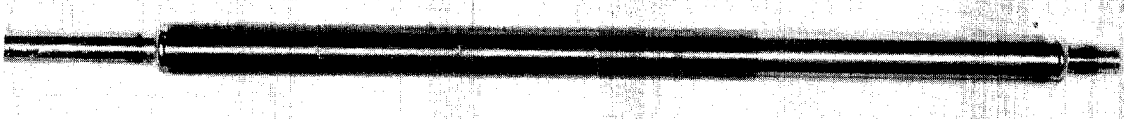

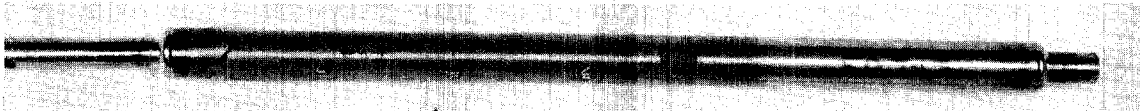
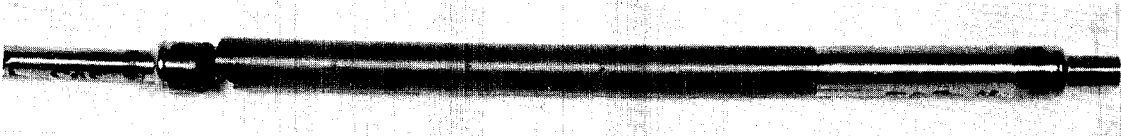

<u>Test No.</u>	<u>Energy Deposition (cal/g.UO₂)</u>
503-2	169
	
503-1	201
	
503-3b	280
	
503-3	283
	
503-4	304
	
503-5	39
	

Fig. 9 (3) Post-test photographs of Cu-barrier fuel rods

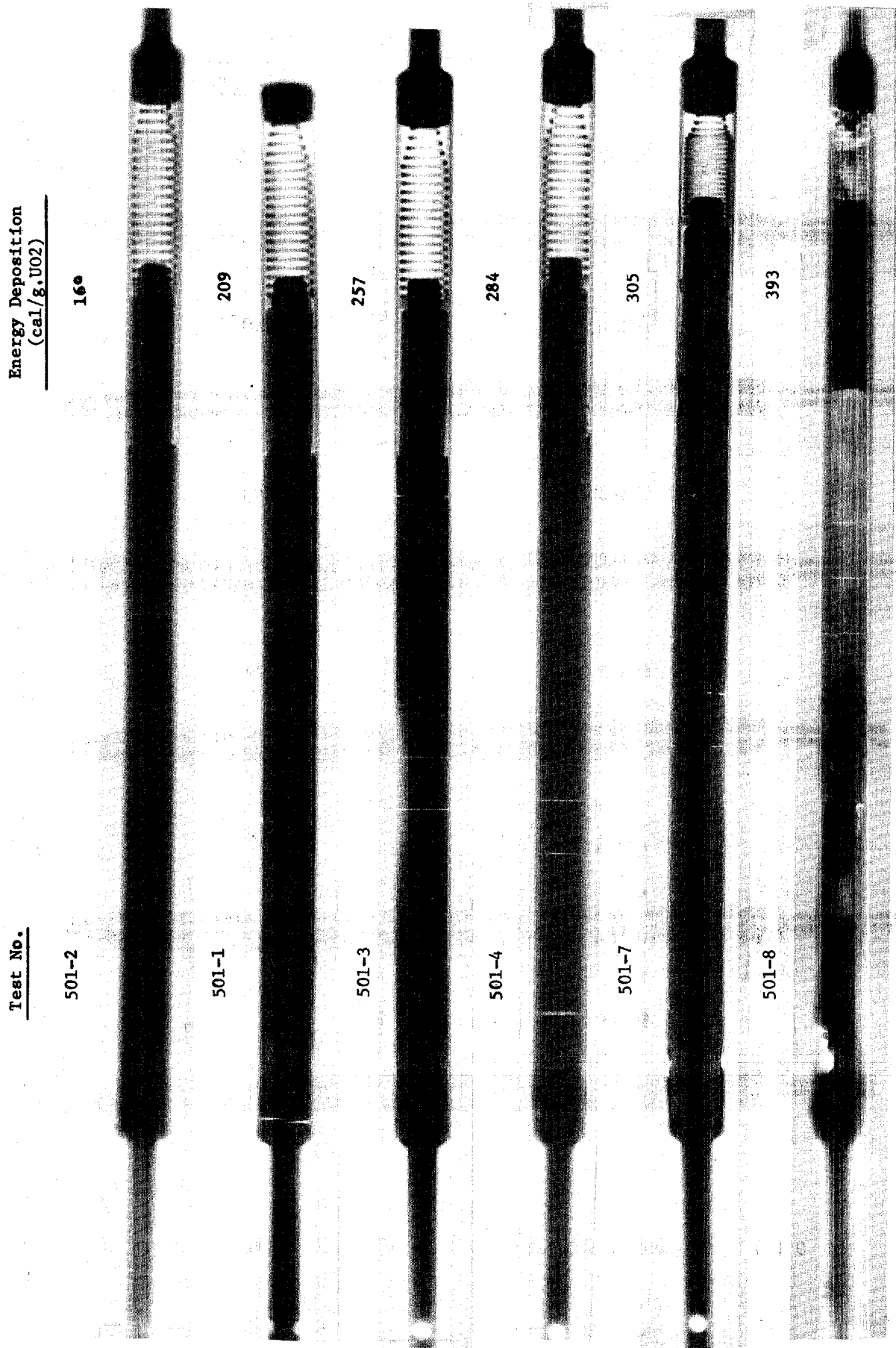


Fig. 10 (1) Post-test X-ray photographs of Reference fuel rods

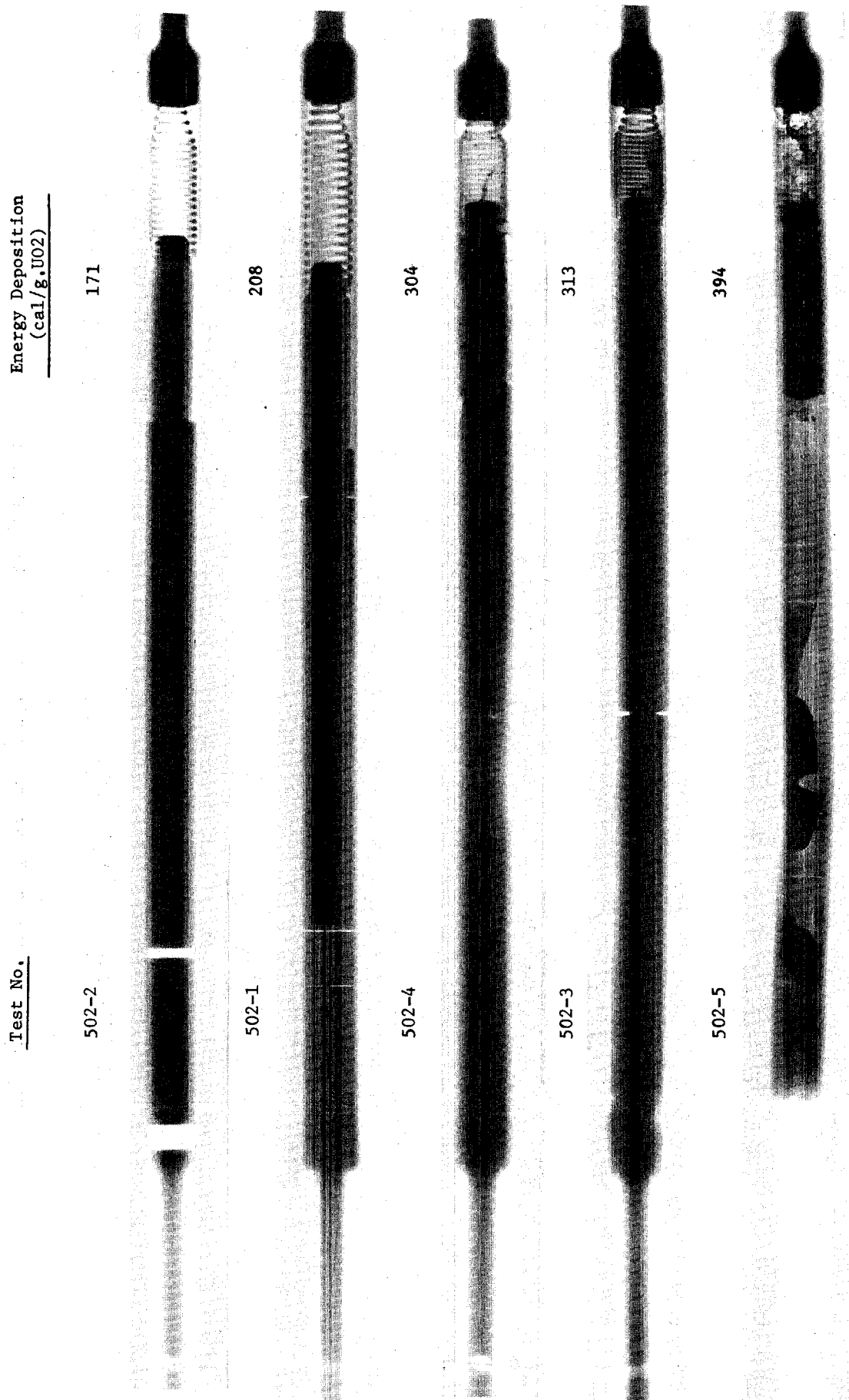


Fig. 10 (2) Post-test X-ray photographs of Zr-lined fuel rods

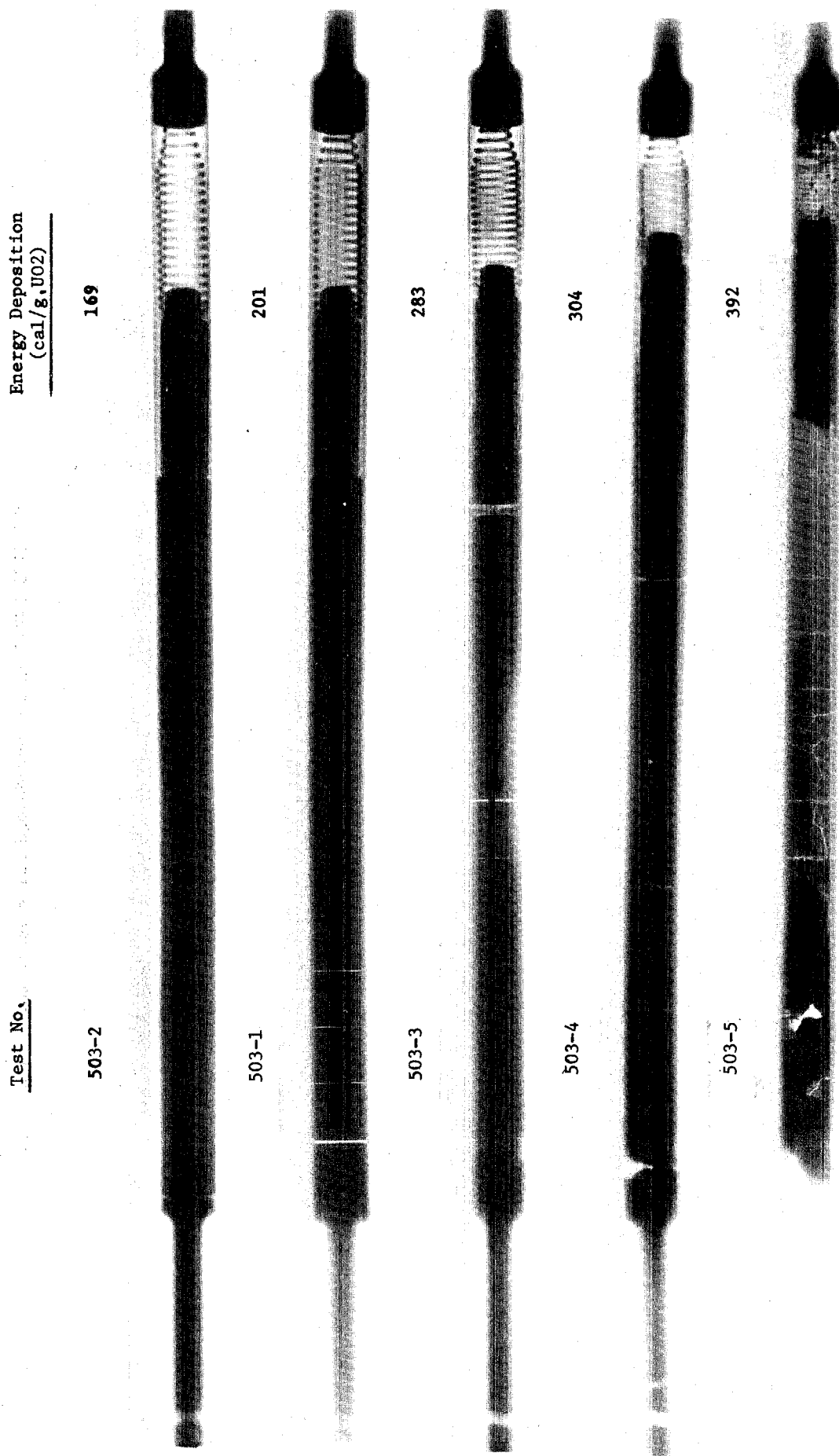


Fig. 10 (3) Post-test X-ray photographs of Cu-barrier fuel rods

Energy Deposition
(cal/g.UO₂)

Test No.

169

501-2

209

501-1

257

501-3

305

501-7

393

501-8

Fig. 11(1) Post-test NRG photographs of Reference fuel rods

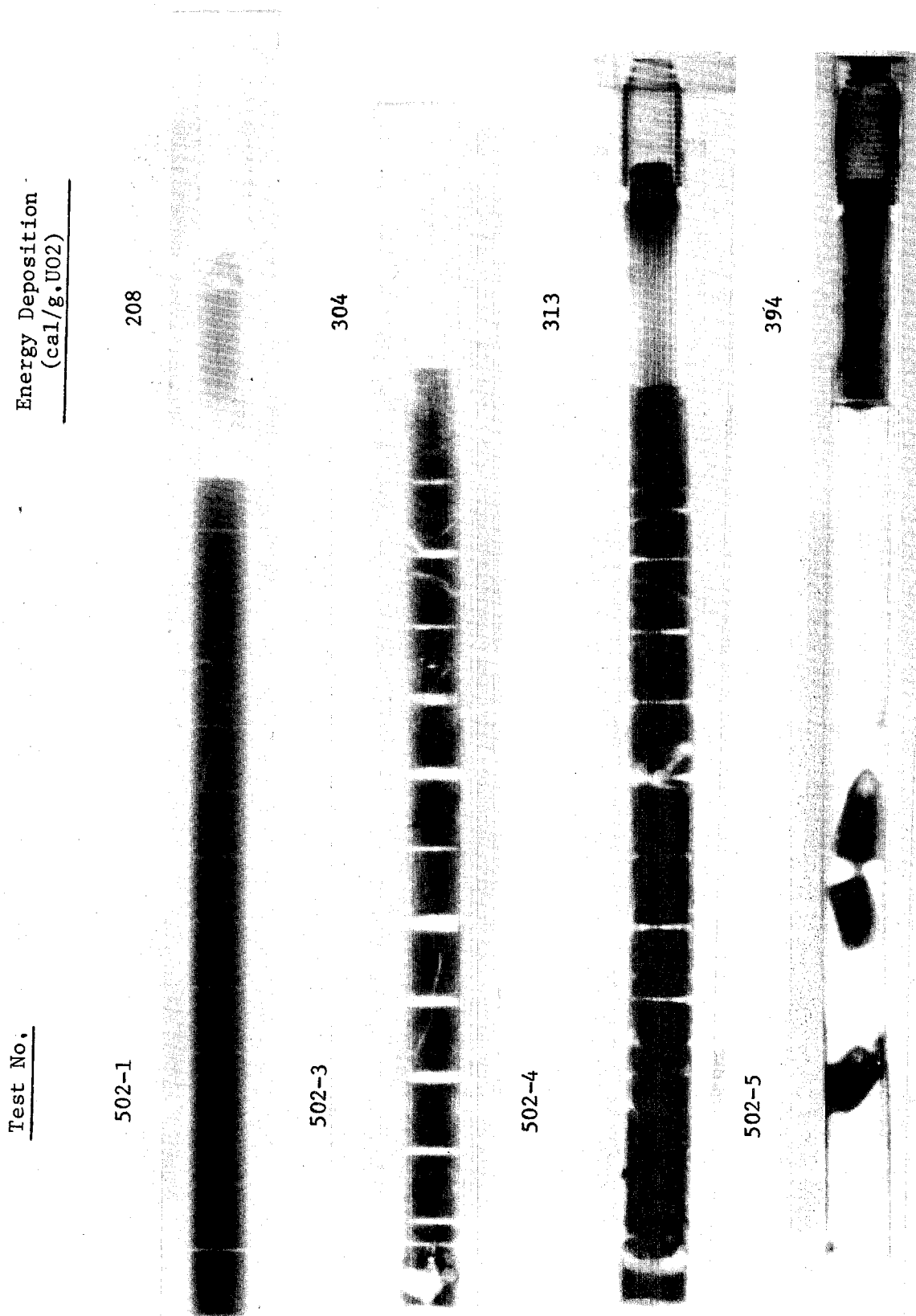


Fig. 11(2) Post-test NRG photographs of Zr-lined fuel rods

Energy Deposition
(cal/g.UO₂)

Test No.

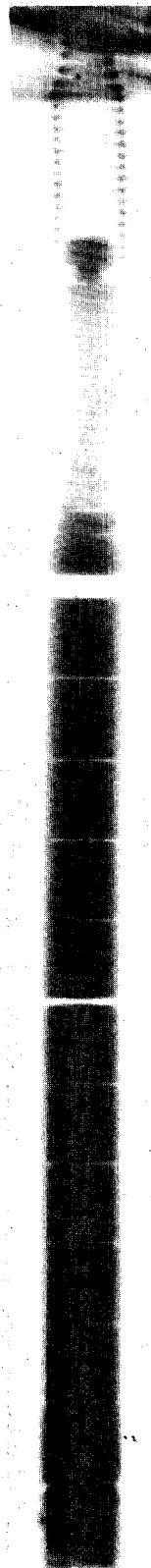
503-1

201



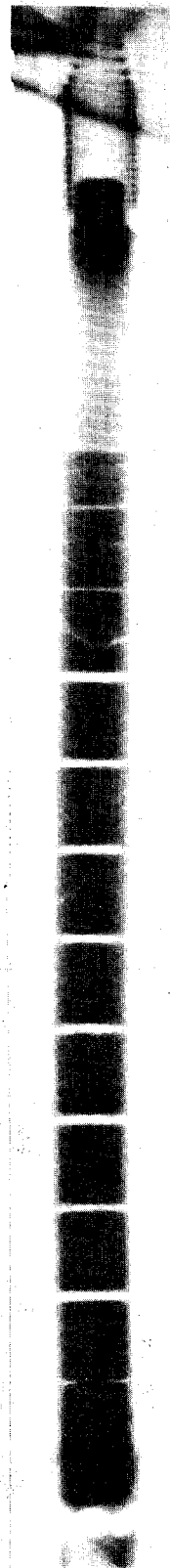
503-3

283



503-4

304



503-5

392



Fig. 11(3) Post-test NRG photographs of Cu-barrier fuel rods

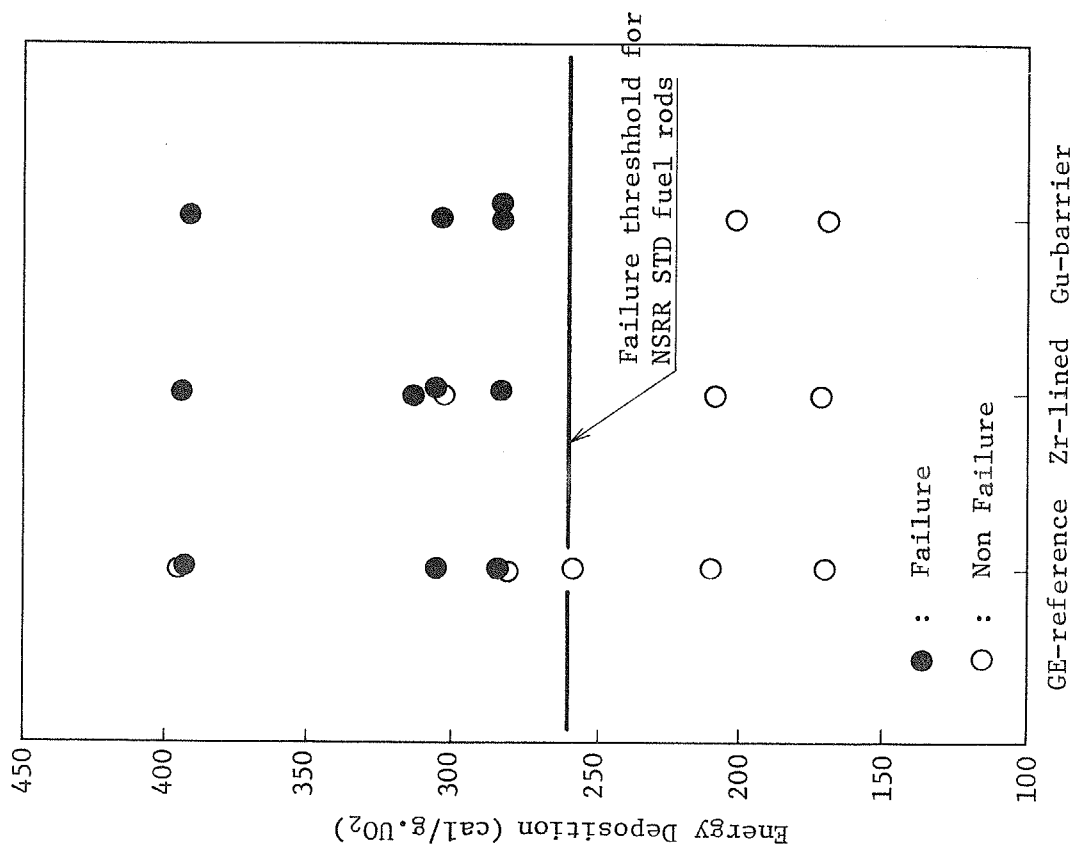


Fig. 12 Comparison of failure threshold for GE fuel rods

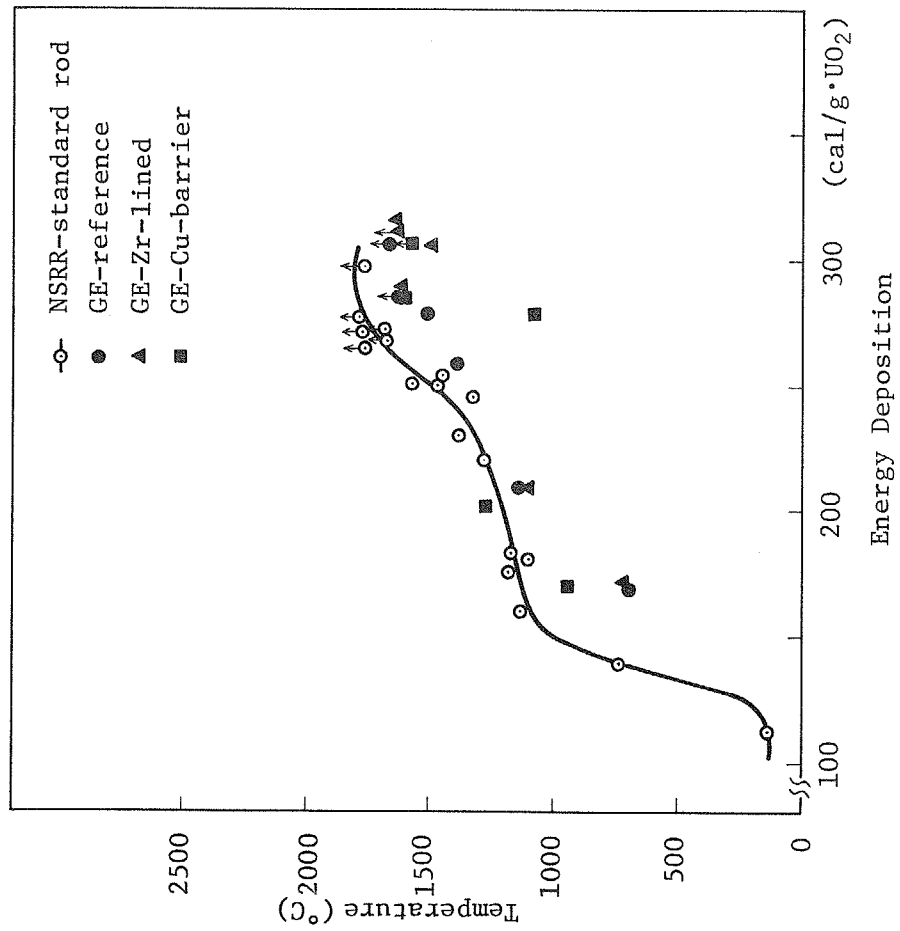


Fig. 13 Max. cladding surface temperature at axial center

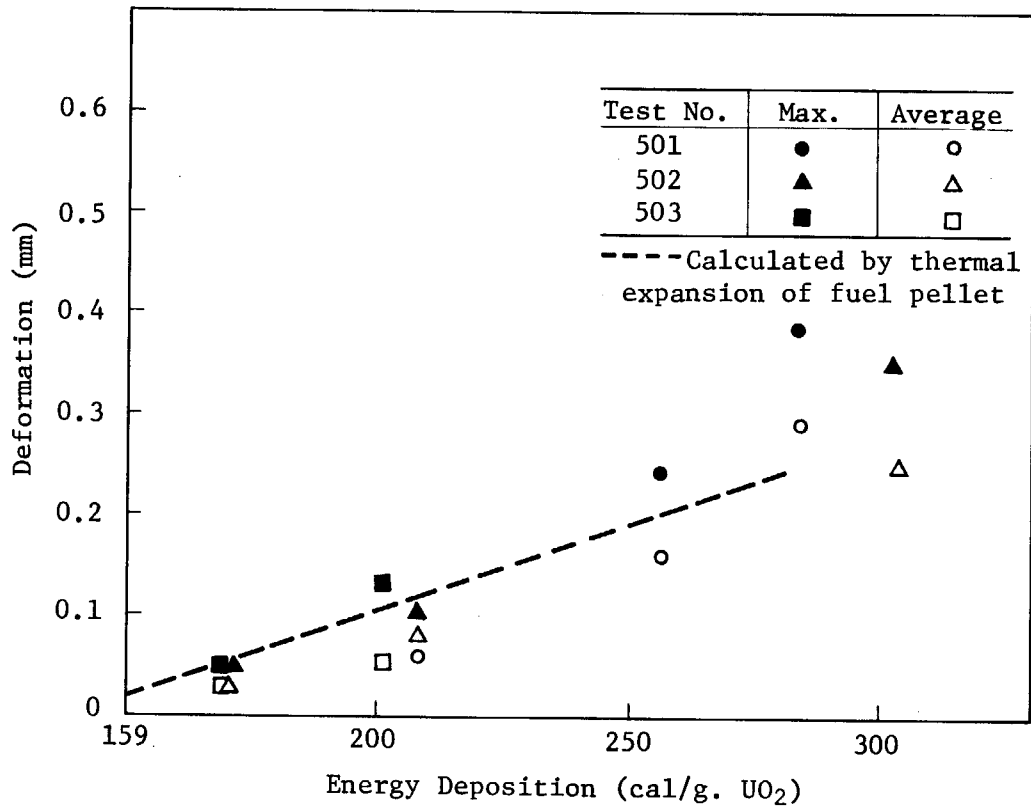


Fig. 14 Max. and averaged radial deformation of fuel rods at axial center of the rod.

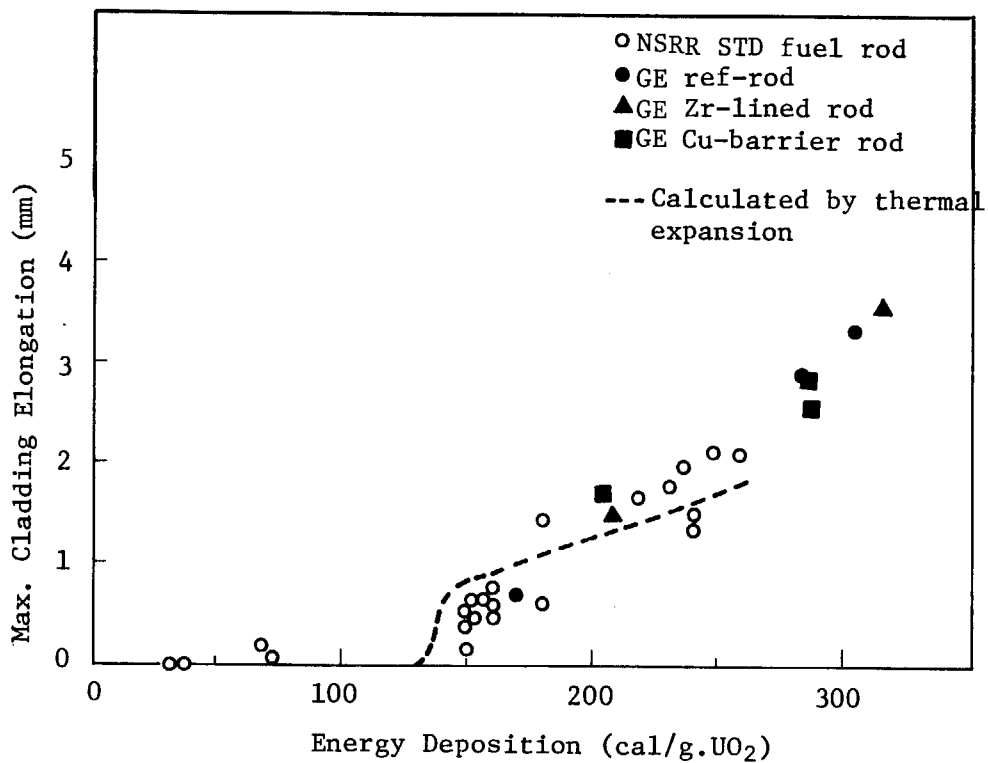


Fig. 15 Max. cladding elongation

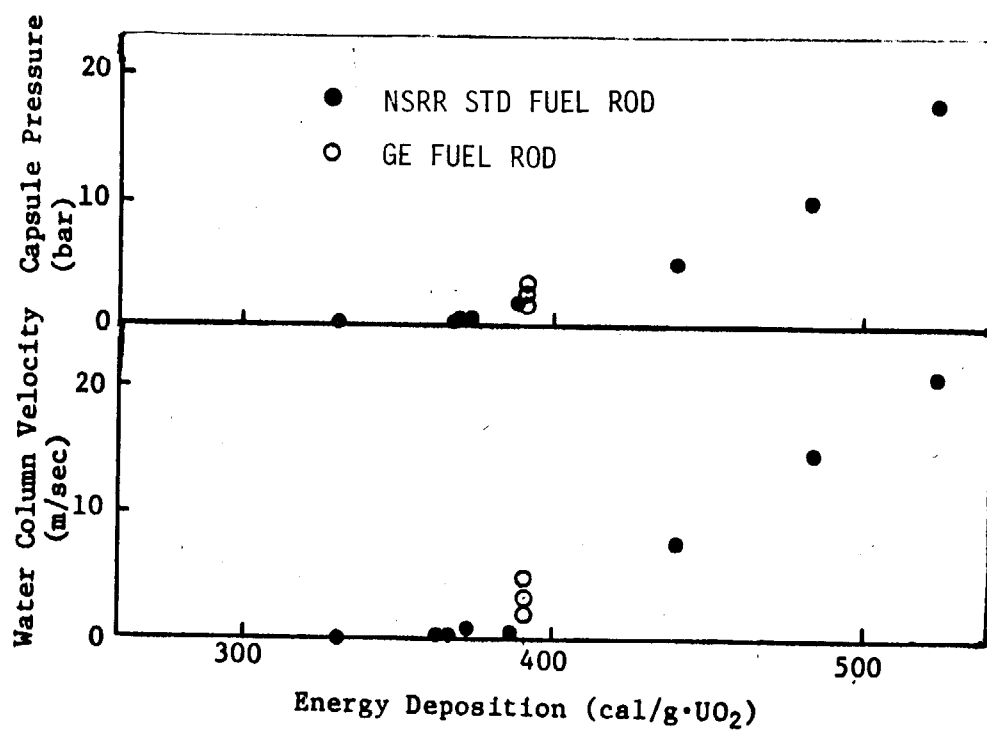
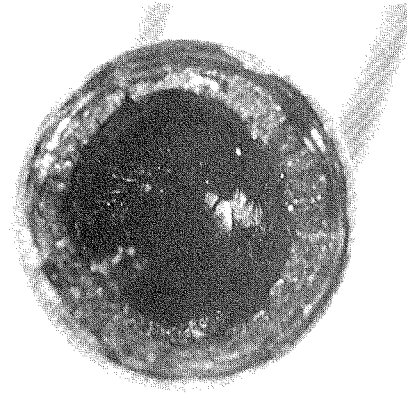
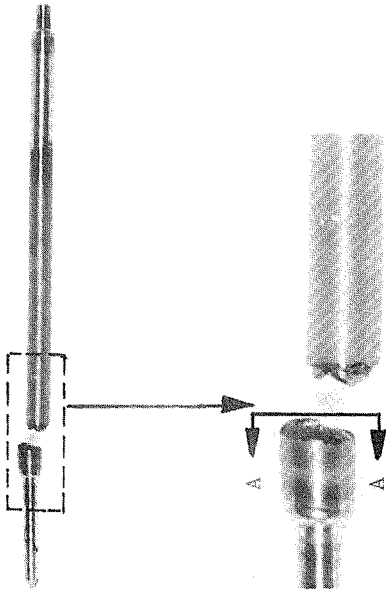


Fig. 16 Energy deposition vs. average water column velocity and max. capsule pressure

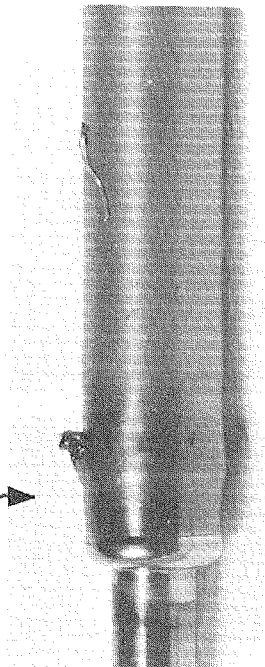
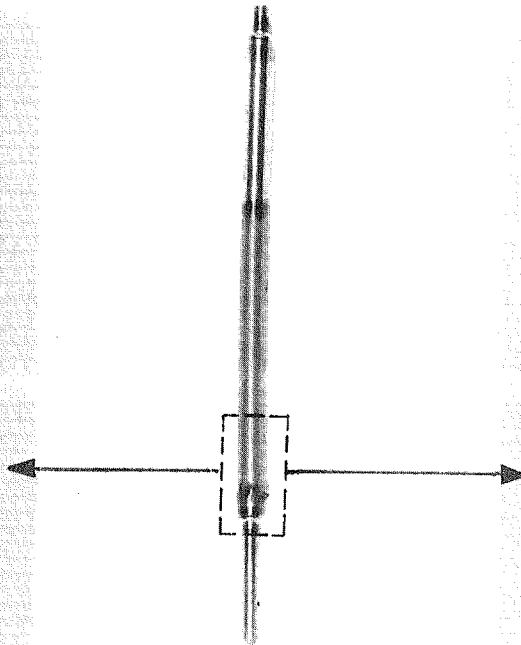
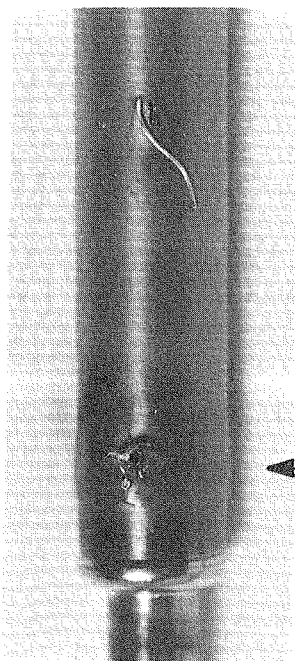
Appendices

- A Magnified views of fuel rods at failed portions
- B Transient records during irradiation
 - B-1 ~15 Cladding surface temperature
 - B-16~18 Water column velocity and capsule internal pressure
 - B-19~25 Cladding elongation
- C Profile measurement of cladding radial deformation
- D NSRR standard fuel rod test
 - D-1 Schema of NSRR standard test fuel rod
 - D-2 Appearance of post-test fuel rods in NSRR standard fuel rod tests related with energy deposition

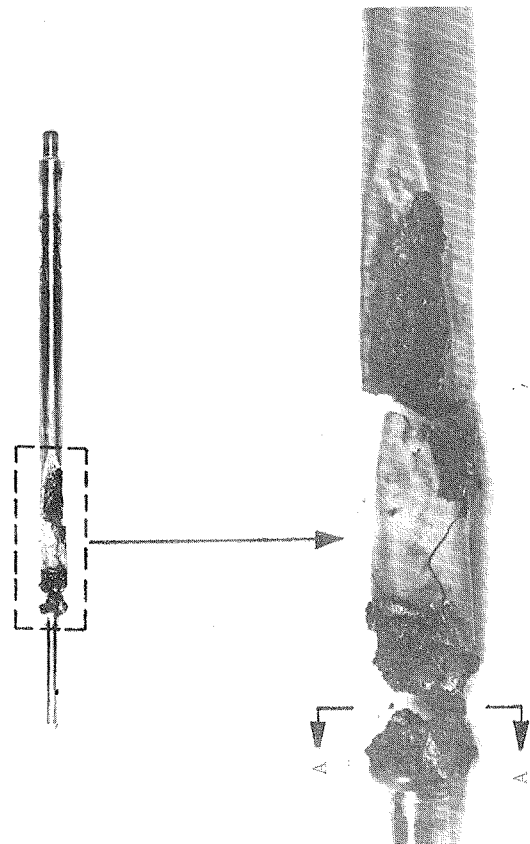


A-A section

A-2 Photographs of the failed portion of a fuel rod in Test No. 501-7 (GE-reference, 305 cal/g·UO₂)

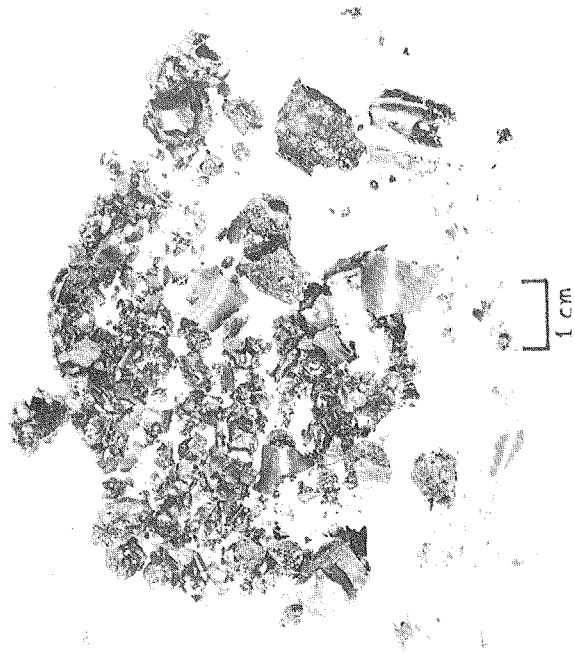
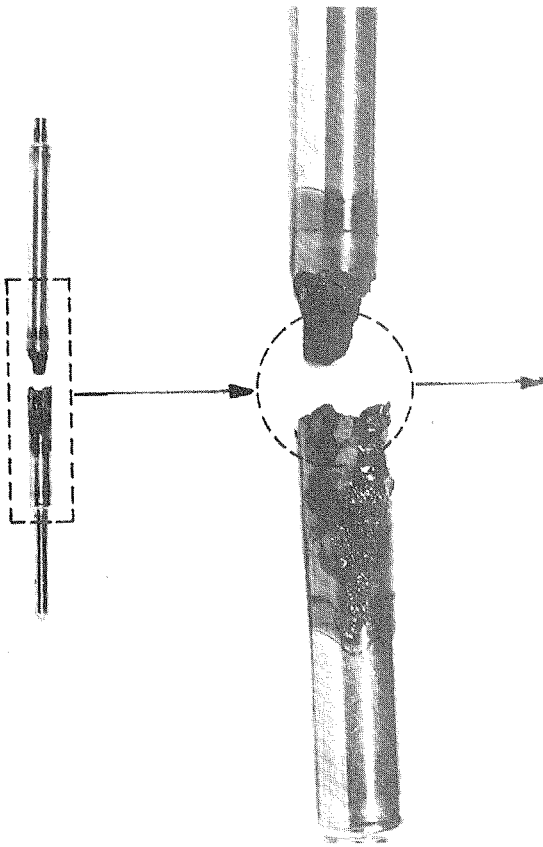


A-1 Photographs of the failed portion of a fuel rod in Test No. 501-4 (GE-reference, 284 cal/g·UO₂)

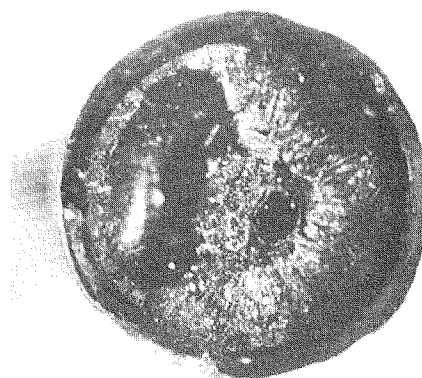
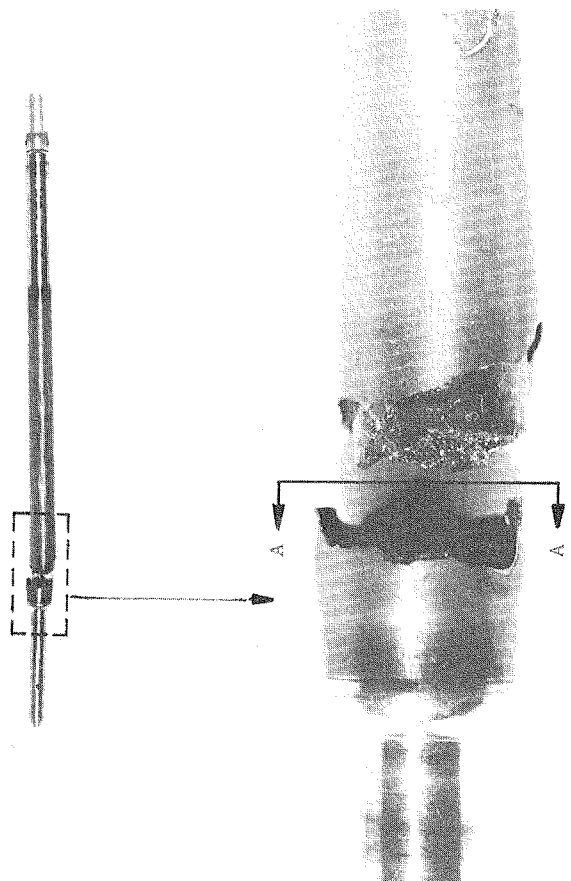


A-A section

A-3 Photographs of the failed portion of a fuel rod in Test No. 501-8 (GE-reference, 393 cal/g·UO₂)

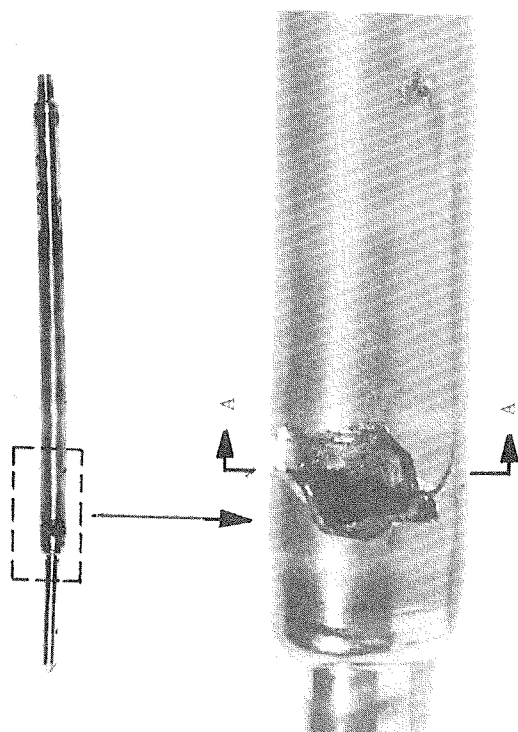


A-4 Photographs of the failed portion of a fuel rod in Test No. 501-9 (GE-reference w/Cd sheet, 394 cal/g·UO₂)



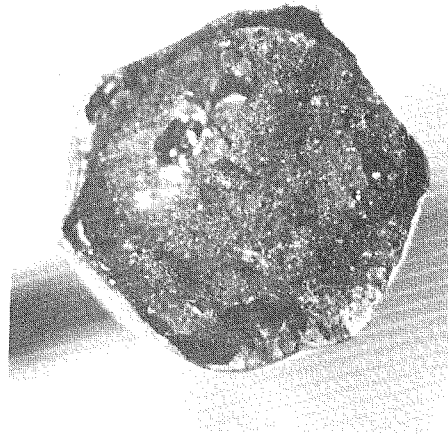
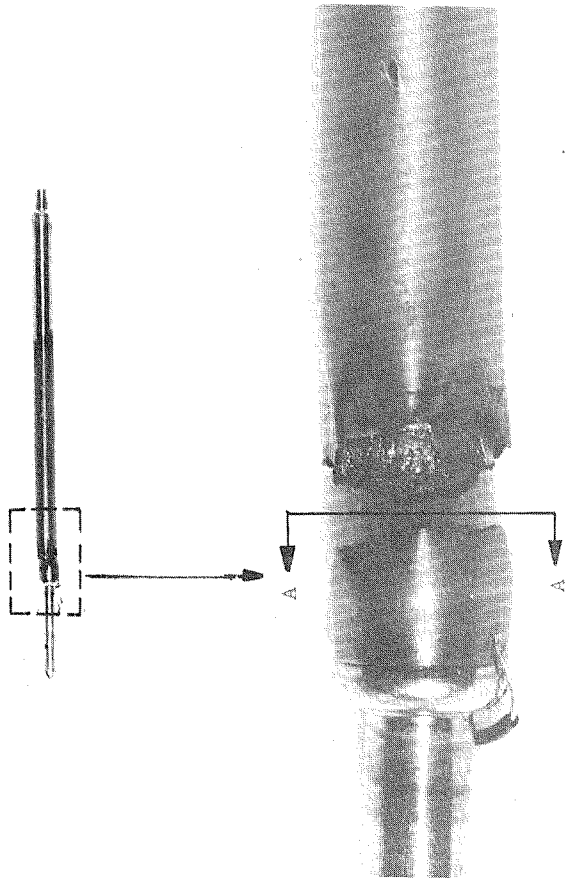
A-A section

A-6 Photographs of the failed portion of a fuel rod in Test No. 502-4B (Zr-lined, 309 cal/g·UO₂)



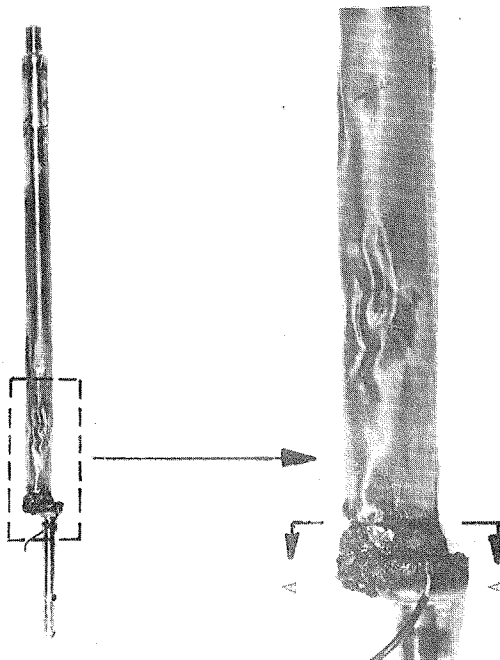
A-A section

A-5 Photographs of the failed portion of a fuel rod in Test No. 502-3 (Zr-lined, 313 cal/g·UO₂)



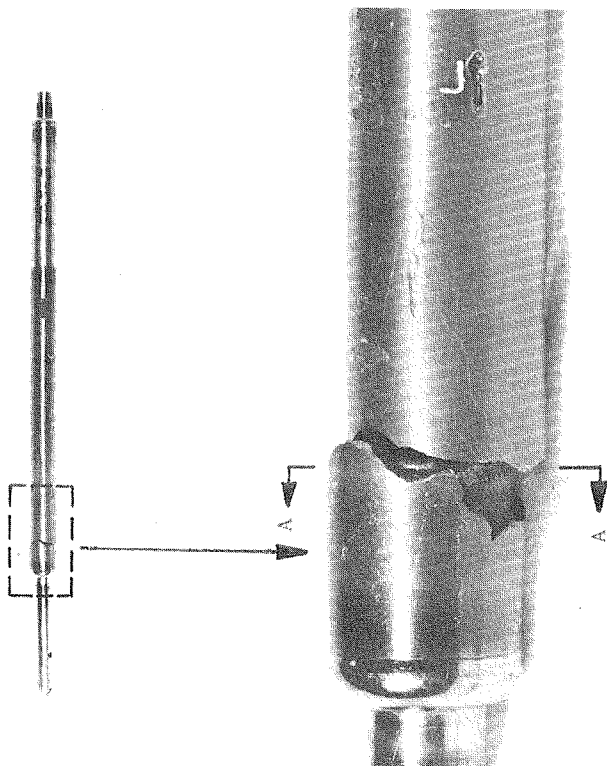
A-A section

A-8 Photographs of the failed portion of a fuel rod in Test No. 502-6 (Zr-lined, 287 cal/g·UO₂)



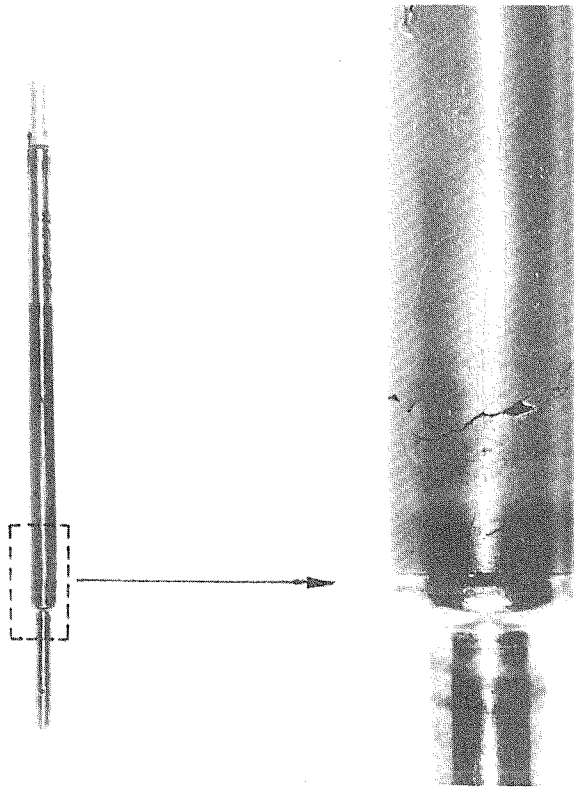
A-A section

A-7 Photographs of the failed portion of a fuel rod in Test No. 502-5 (Zr-lined, 394 cal/g·UO₂)

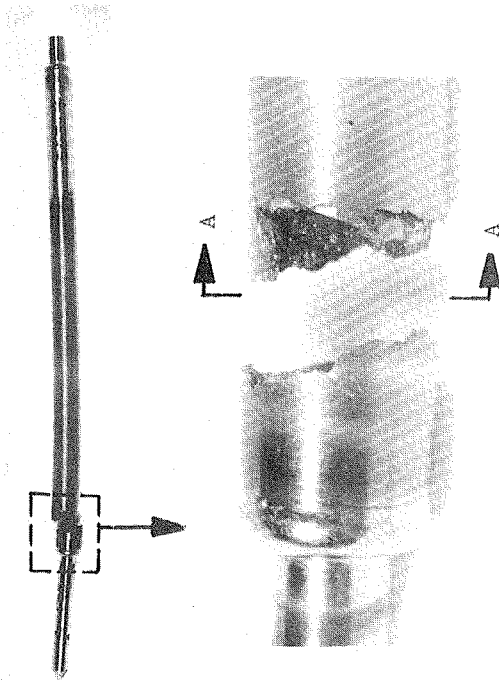


A-A section

A-9 Photographs of the failed portion of a fuel rod in Test No. 503-3 (Cu-barrier, 283 cal/g·UO₂)

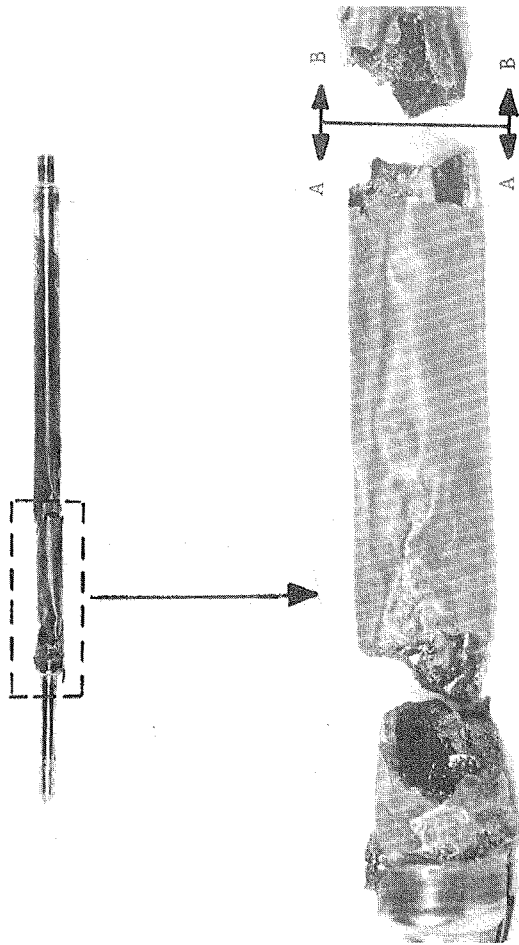


A-10 Photographs of the failed portion of a fuel rod in Test No. 503-3B (Cu-barrier, 280 cal/g·UO₂)



A-A section

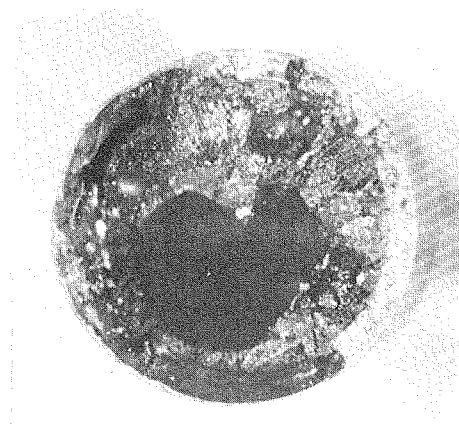
A-11 Photographs of the failed portion of a fuel rod in Test No. 503-4 (Cu-barrier, 304 cal/g·UO₂)

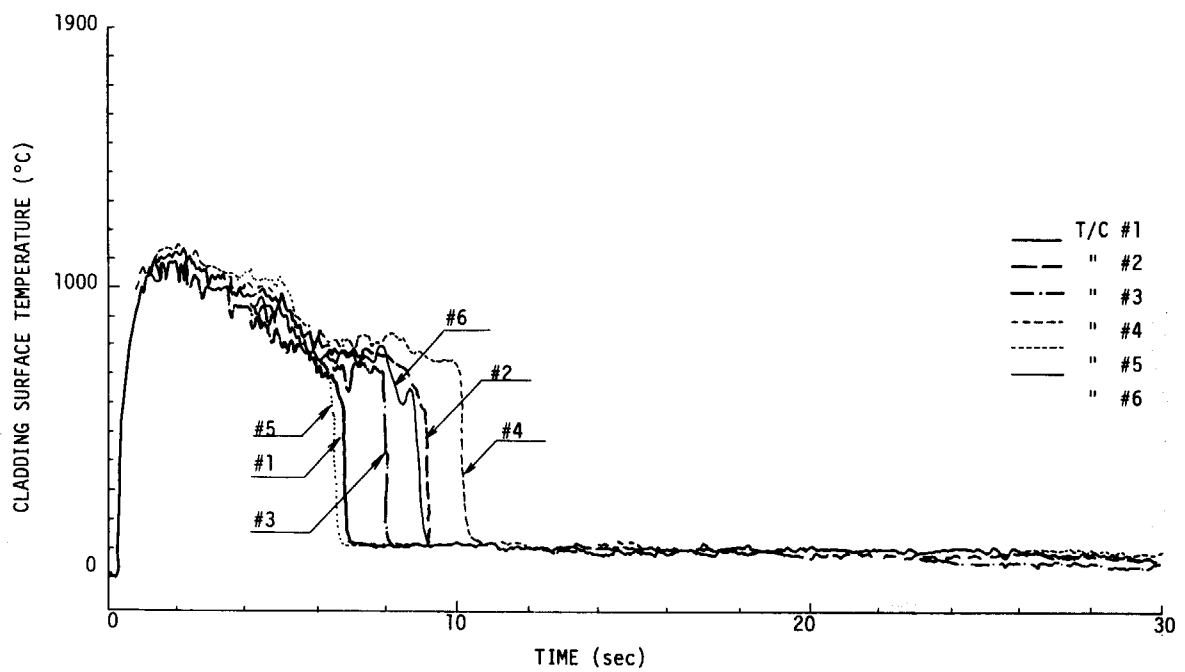


A-A section

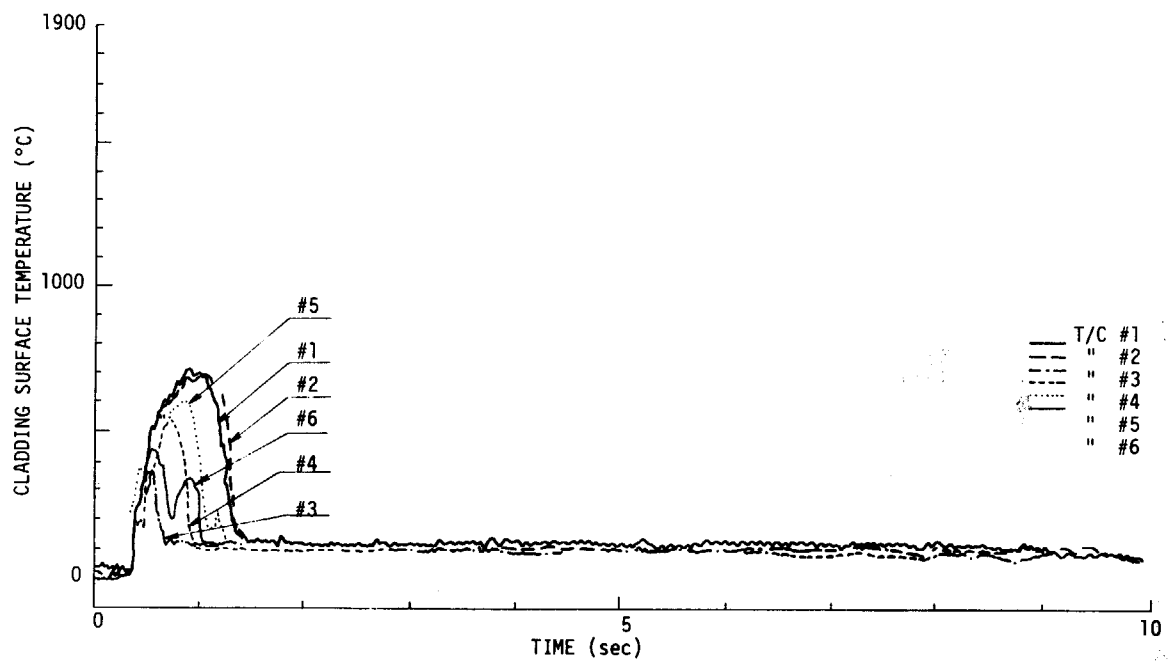
B-B section

A-12 Photographs of the failed portion of a fuel rod in Test No. 503-5 (Cu-barrier, 392 cal/g·UO₂)

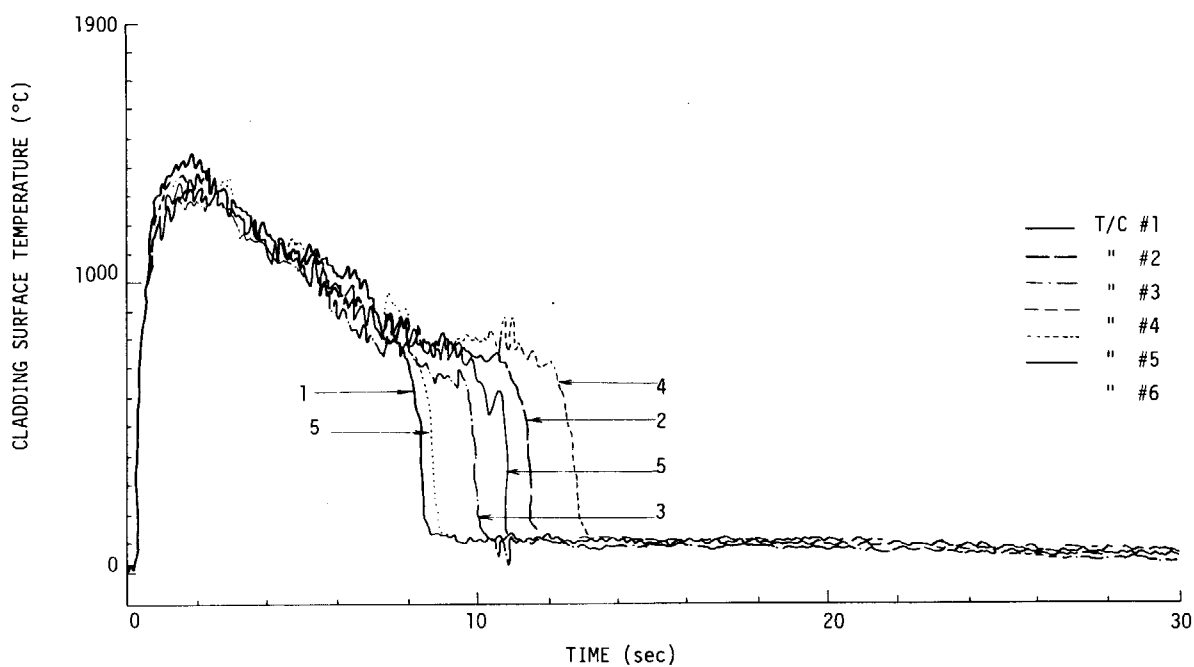




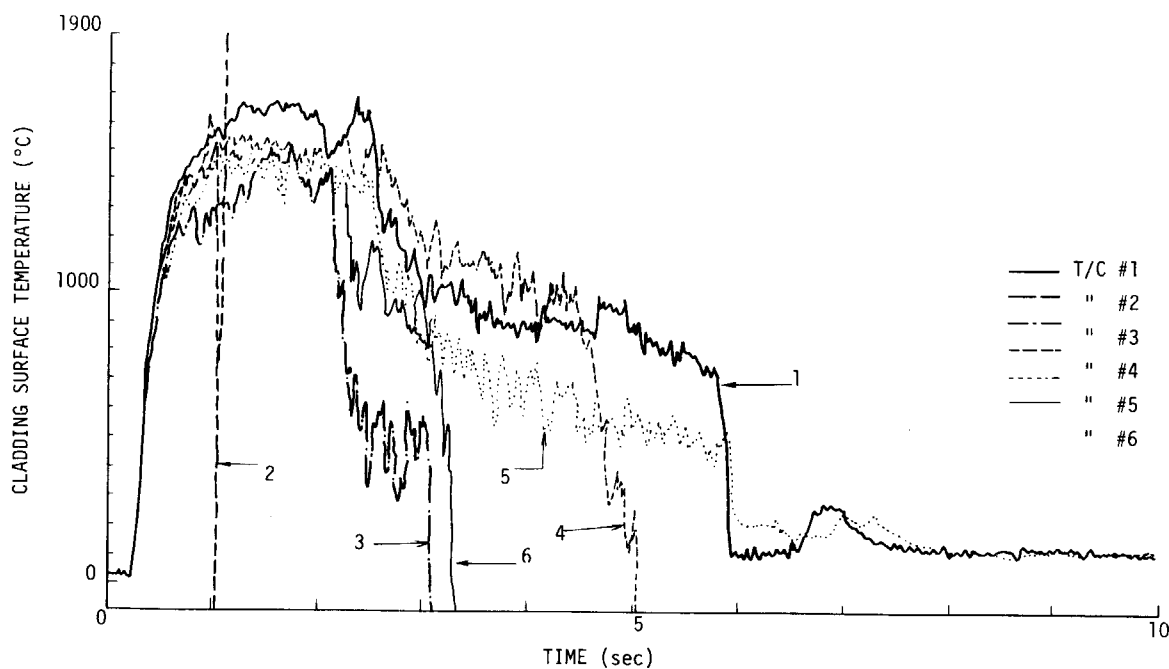
B-1 Transient records of cladding surface temperatures in
Test No. 501-1 (Reference rod, 209 cal/g.UO₂)



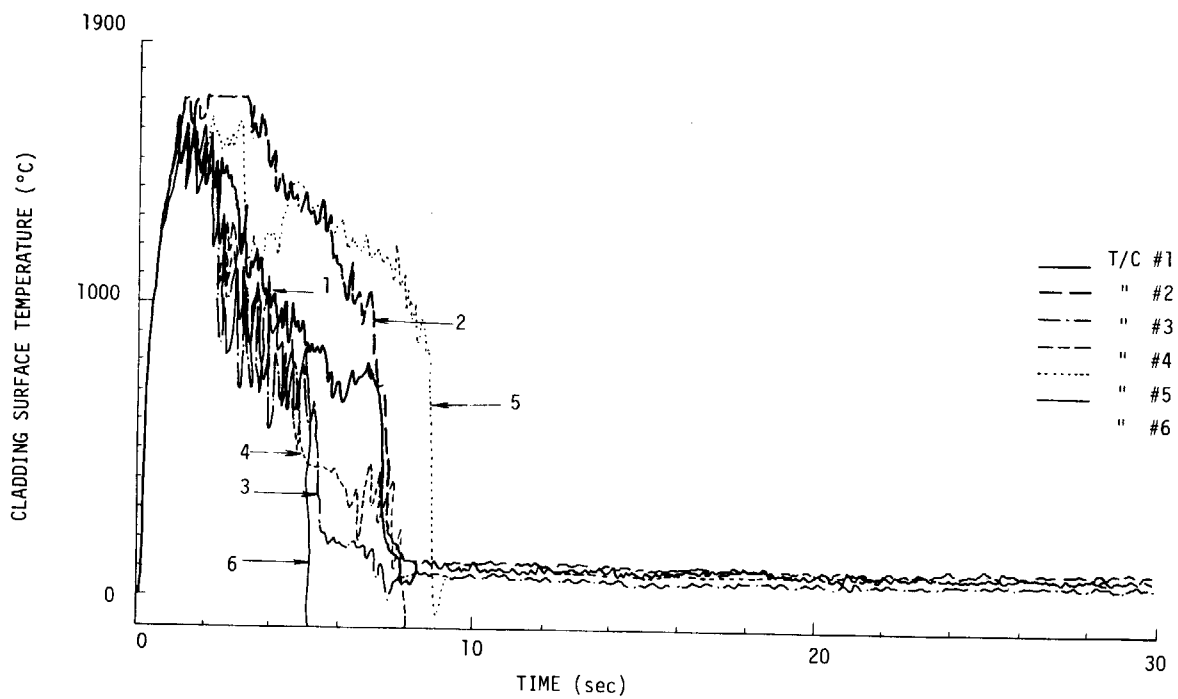
B-2 Transient records of cladding surface temperatures in
Test No. 501-2 (Reference rod, 169 cal/g.UO₂)



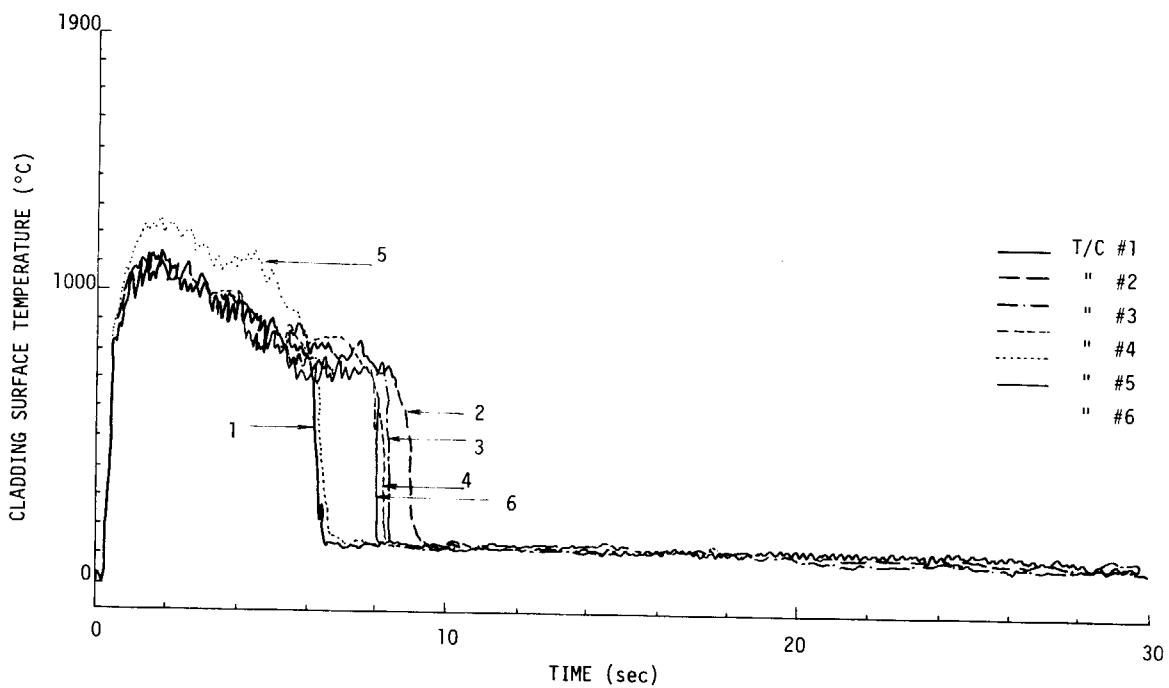
B-3 Transient records of cladding surface temperatures in
Test No. 501-3 (Reference rod, 257 cal/g.UO₂)



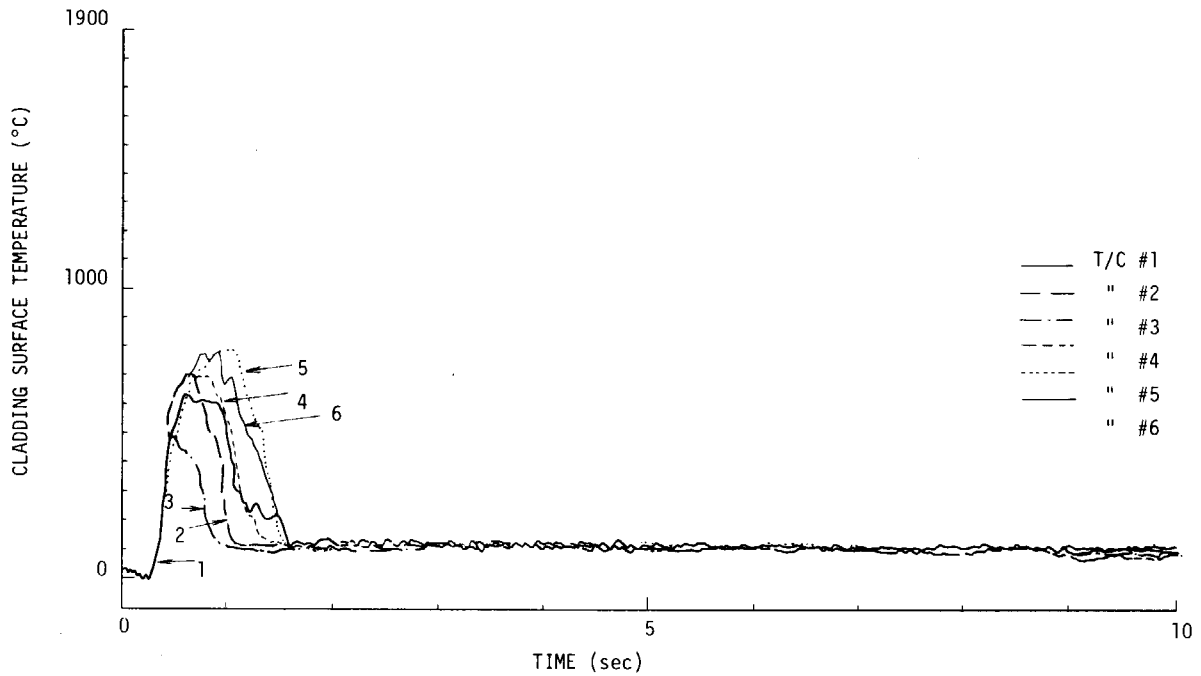
B-4 Transient records of cladding surface temperatures in
Test No. 501-4 (Reference rod, 284 cal/g.UO₂)



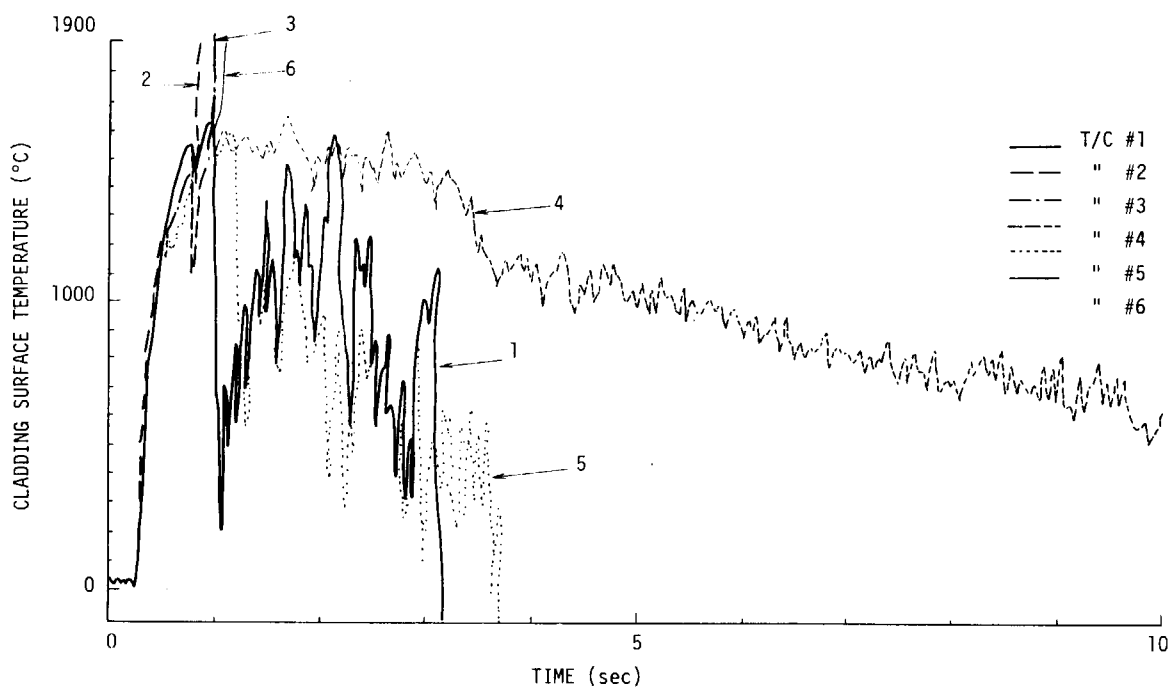
B-5 Transient records of cladding surface temperatures in
Test No. 501-7 (Reference rod, 305 cal/g.UO₂)



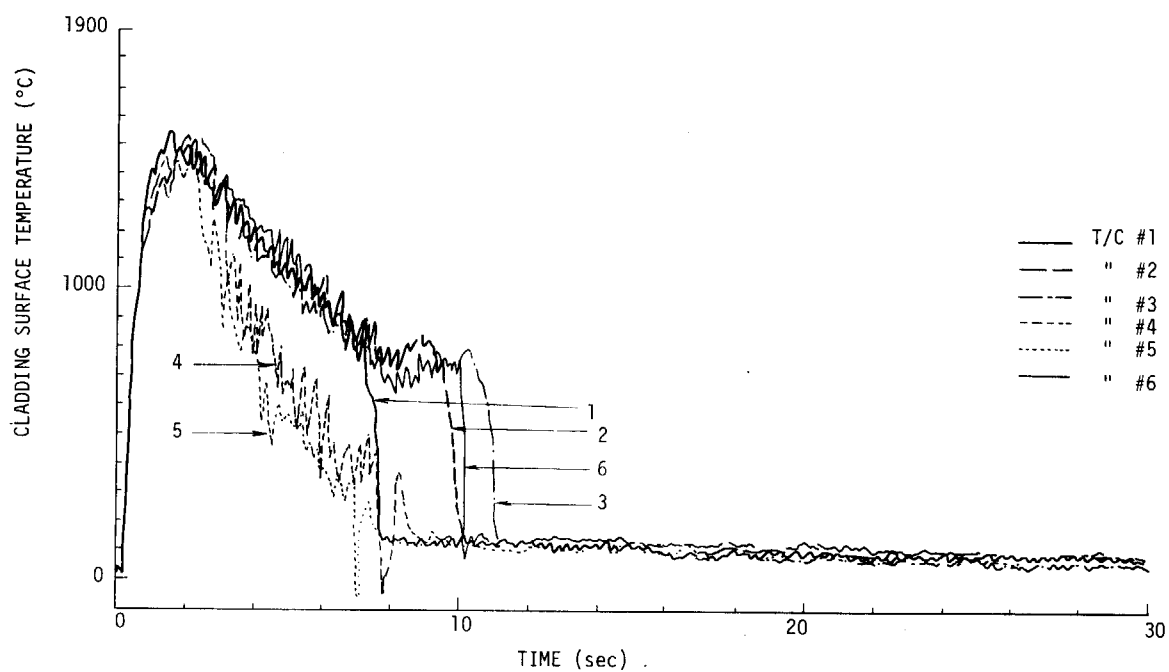
B-6 Transient records of cladding surface temperatures in
Test No. 502-1 (Zr-lined rod, 208 cal/g.UO₂)



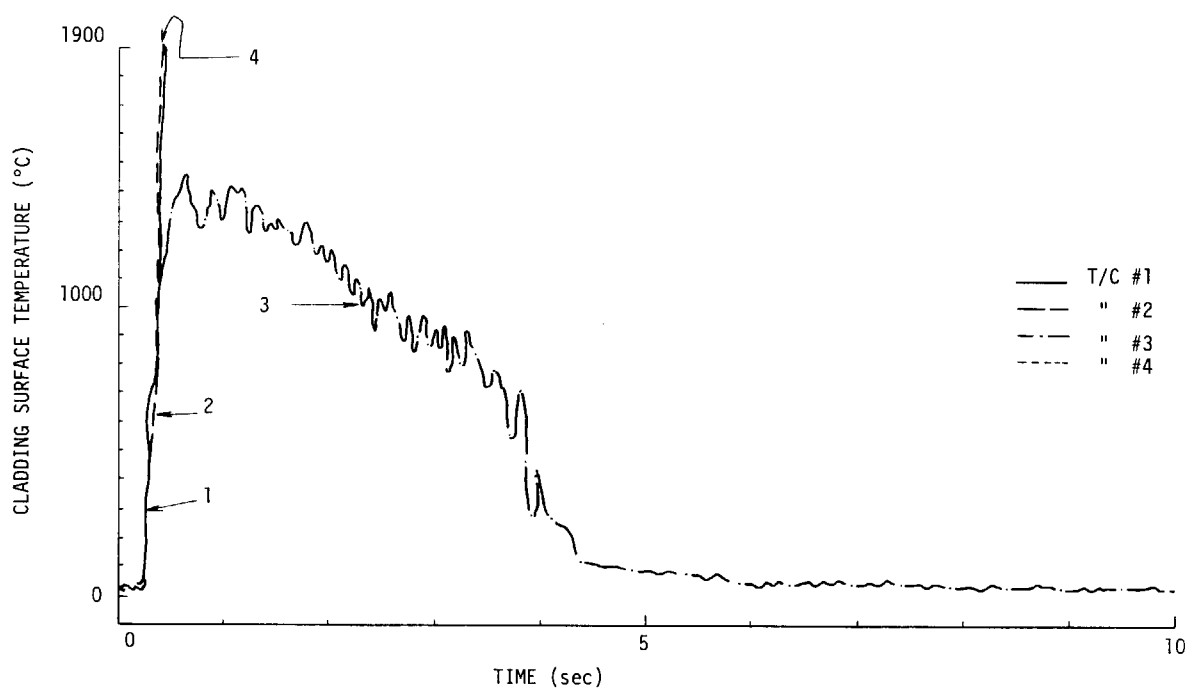
B-7 Transient records of cladding surface temperatures in
Test No. 502-2 (Zr-lined rod, 171 cal/g.UO₂)



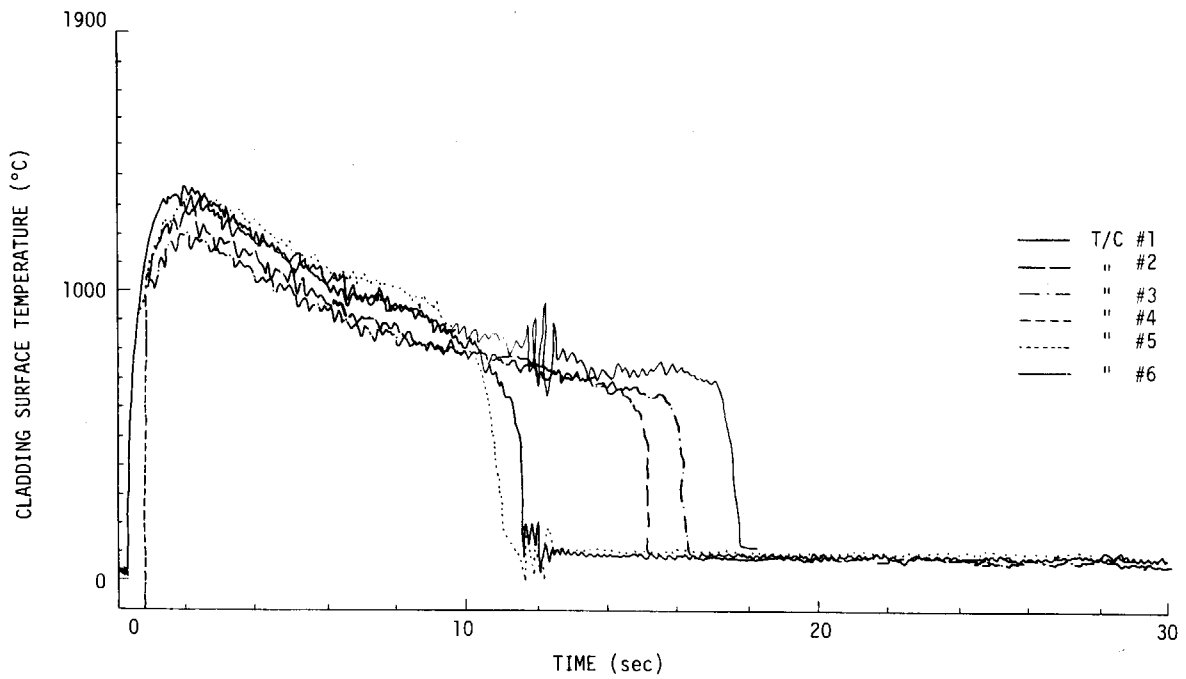
B-8 Transient records of cladding surface temperatures in
Test No. 502-3 (Zr-lined rod, 313 cal/g.UO₂)



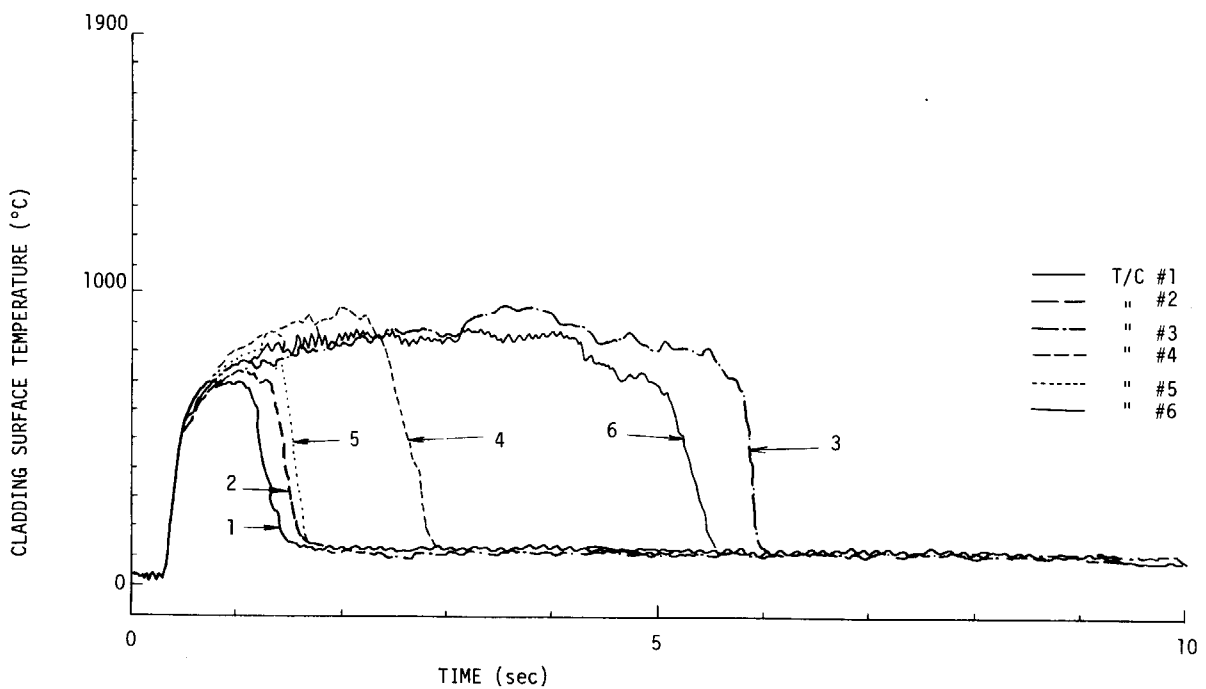
B-9 Transient records of cladding surface temperatures in
Test No. 502-4 (Zr-lined rod, 304 cal/g.UO₂)



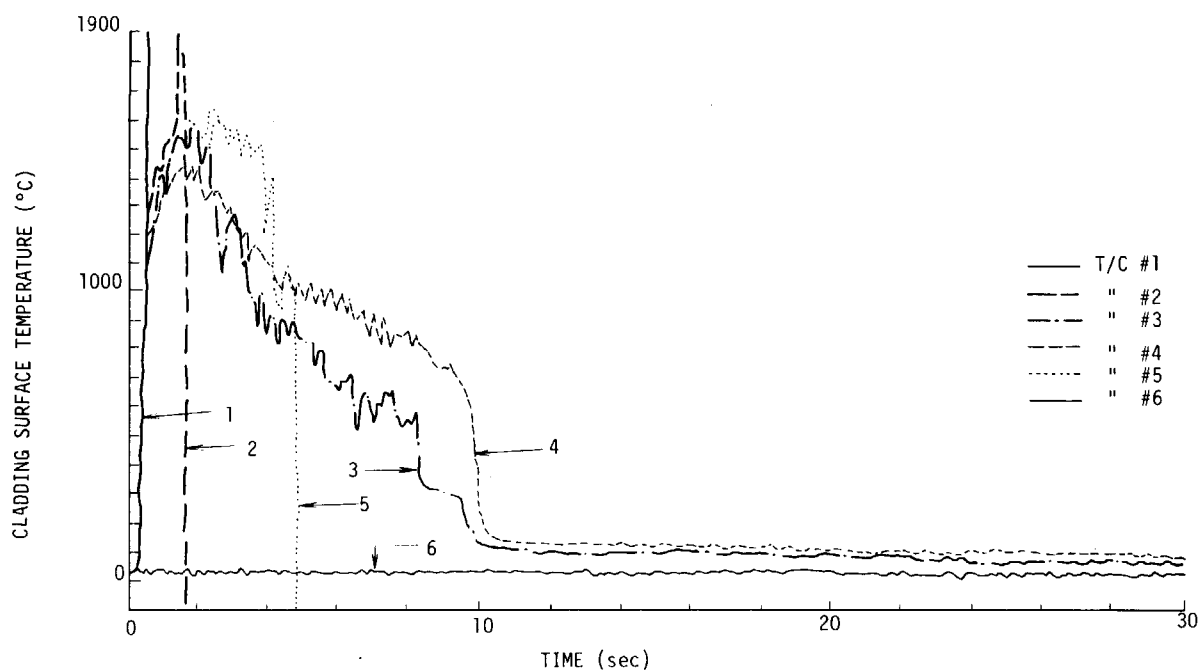
B-10 Transient records of cladding surface temperatures in
Test No. 502-5 (Zr-lined rod, 394 cal/g.UO₂)



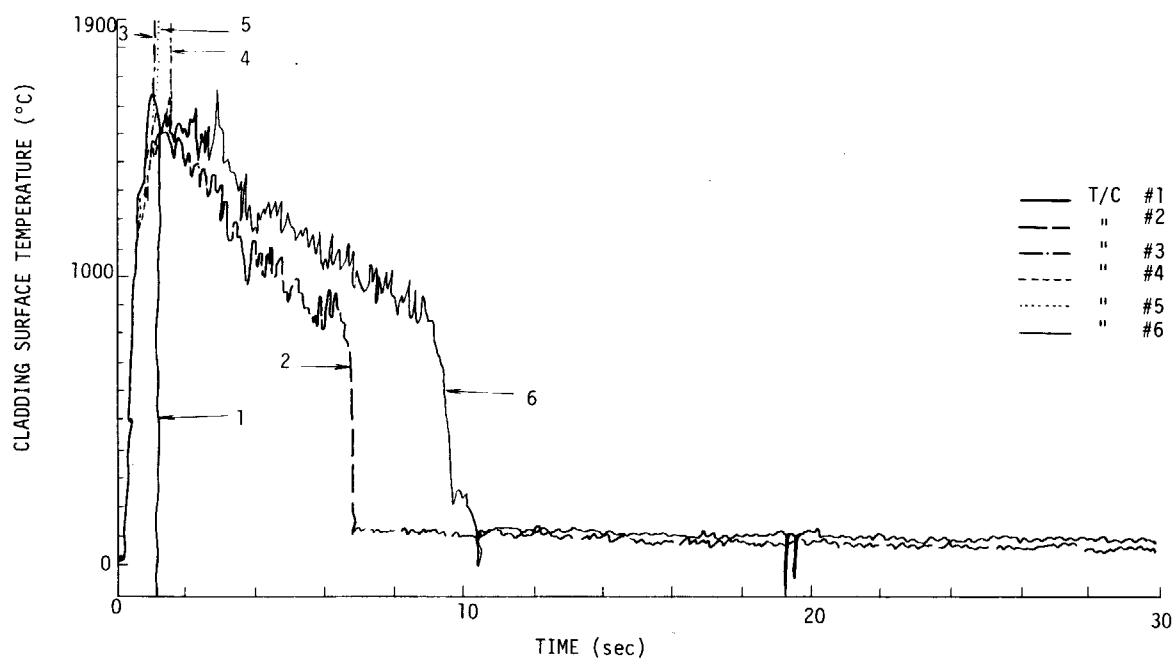
B-11 Transient records of cladding surface temperatures in
Test No. 503-1 (Cu-barrier rod, 201 cal/g.UO₂)



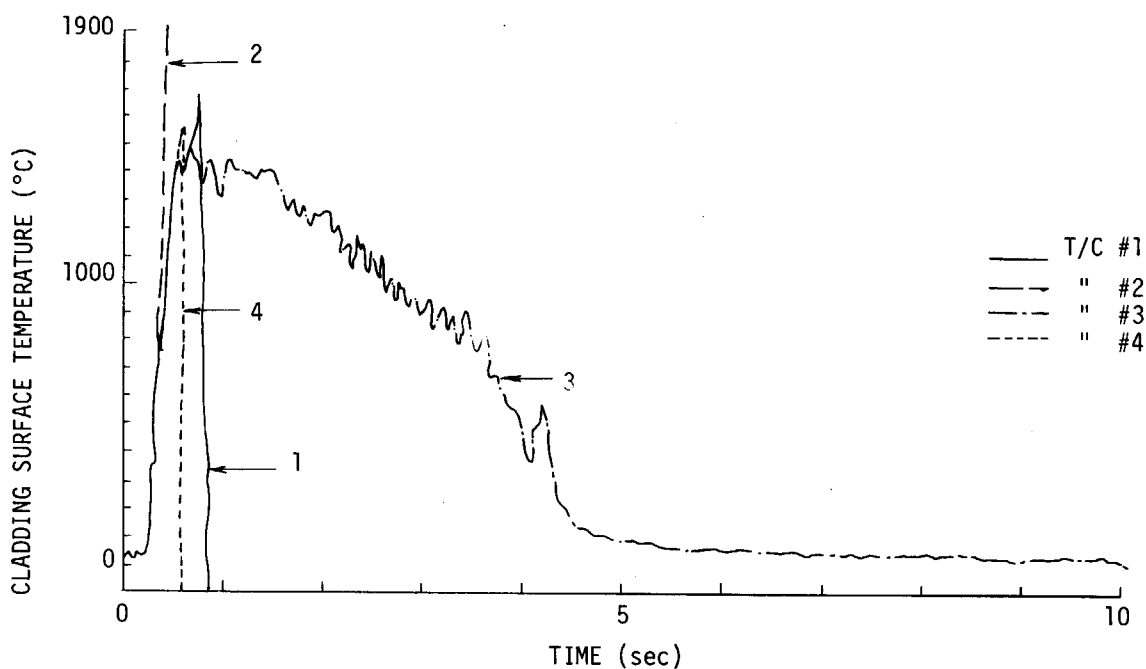
B-12 Transient records of cladding surface temperatures in
Test No. 503-2 (Cu-barrier rod, 169 cal/g.UO₂)



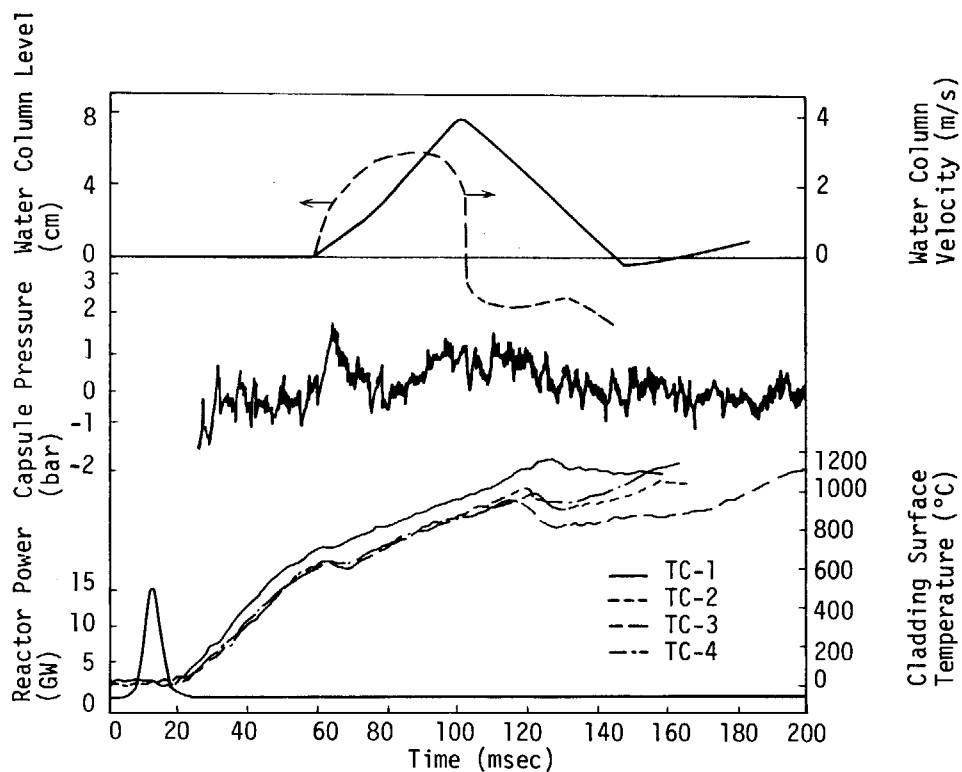
B-13 Transient records of cladding surface temperatures in
Test No. 503-3 (Cu-barrier rod, 283 cal/g.UO₂)



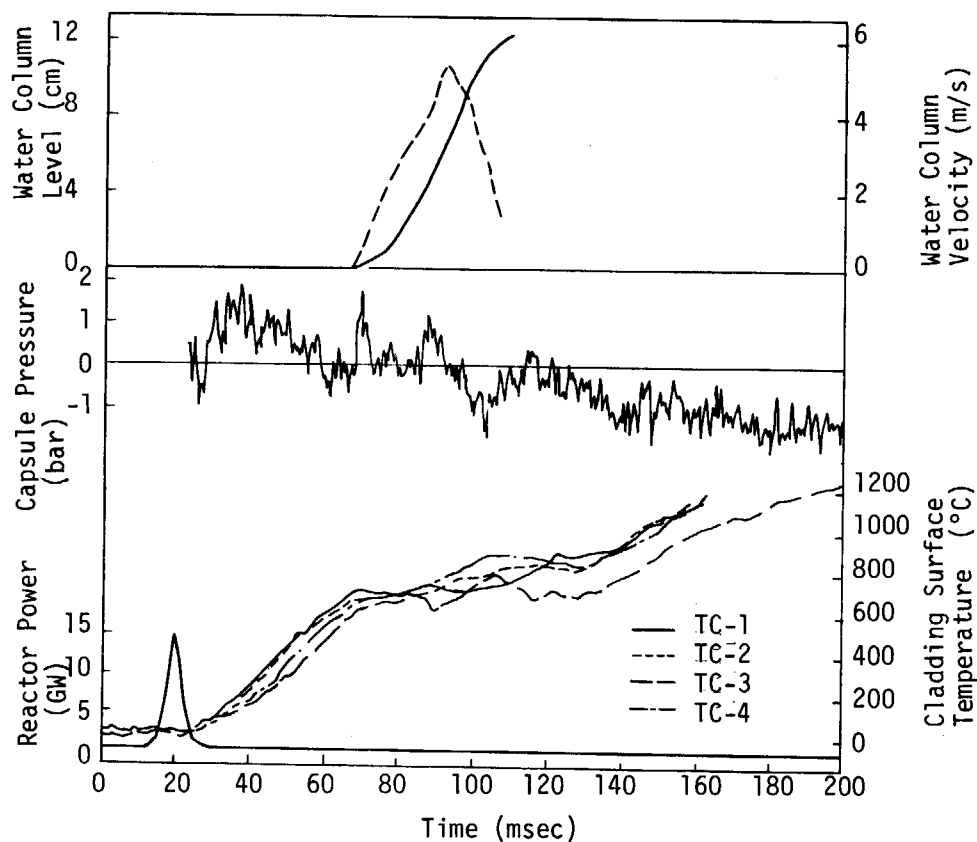
B-14 Transient records of cladding surface temperatures in
Test No. 503-4 (Cu-barrier rod, 304 cal/g.UO₂)



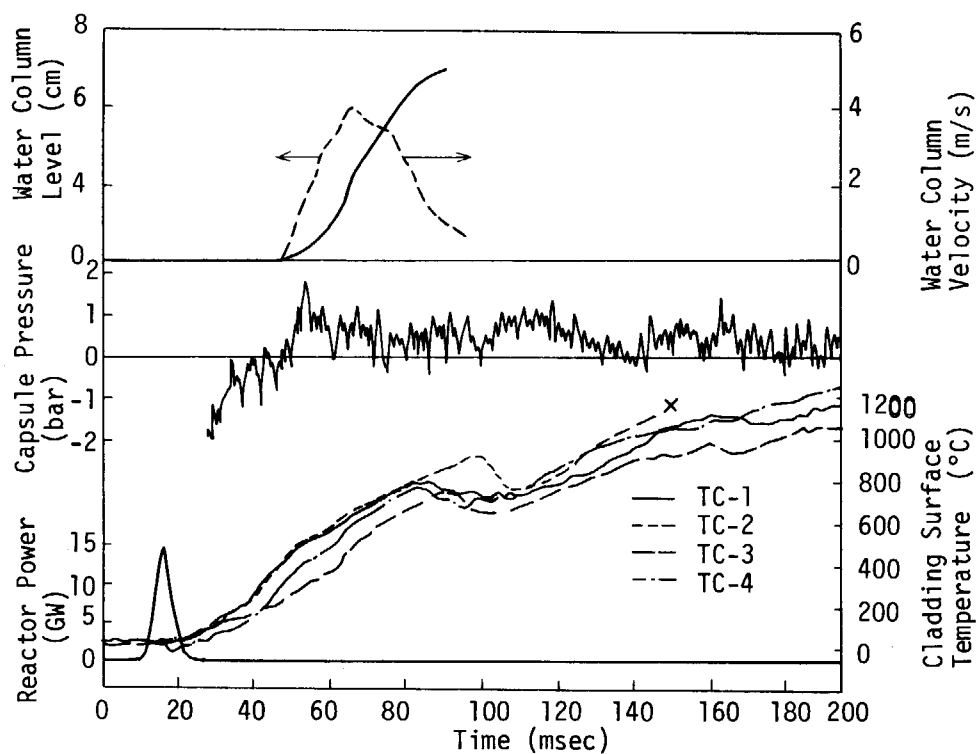
B-15 Transient records of cladding surface temperatures in Test No. 503-5 (Cu-barrier rod, 392 cal/g.UO₂)



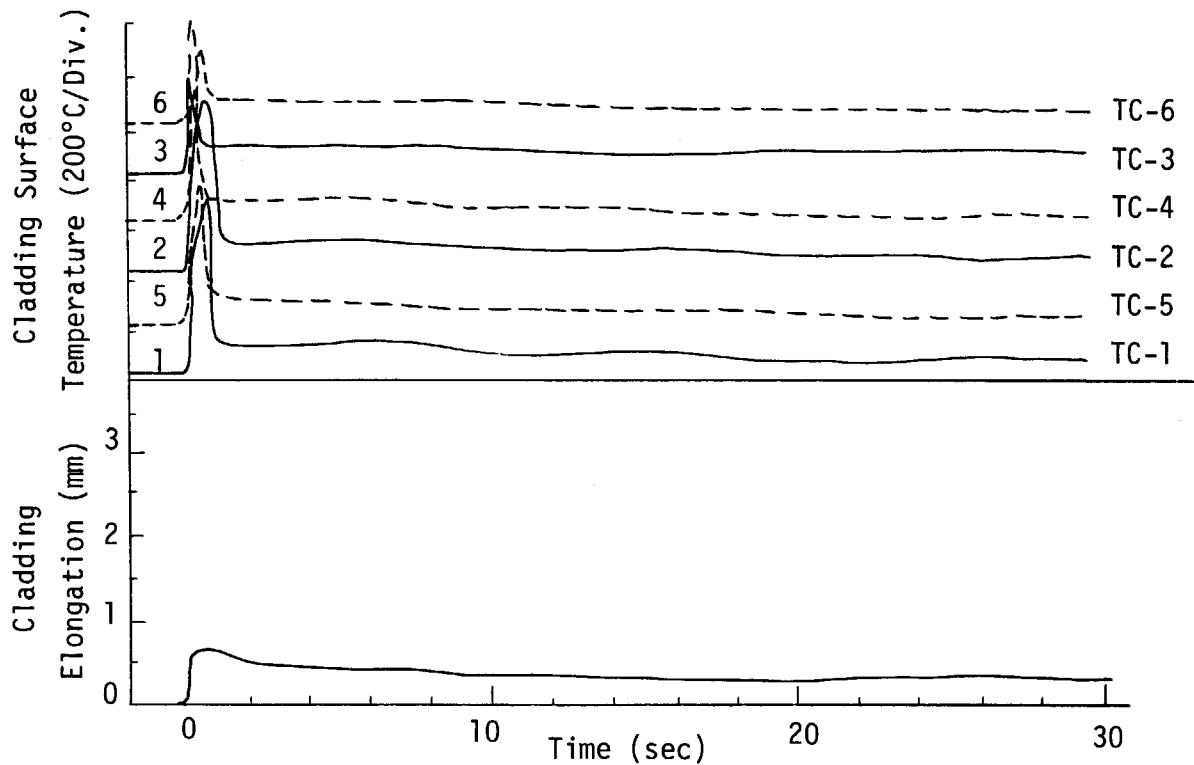
B-16 Transient records of Test No. 501-8 (GE-reference rod, 393 cal/g.UO₂)



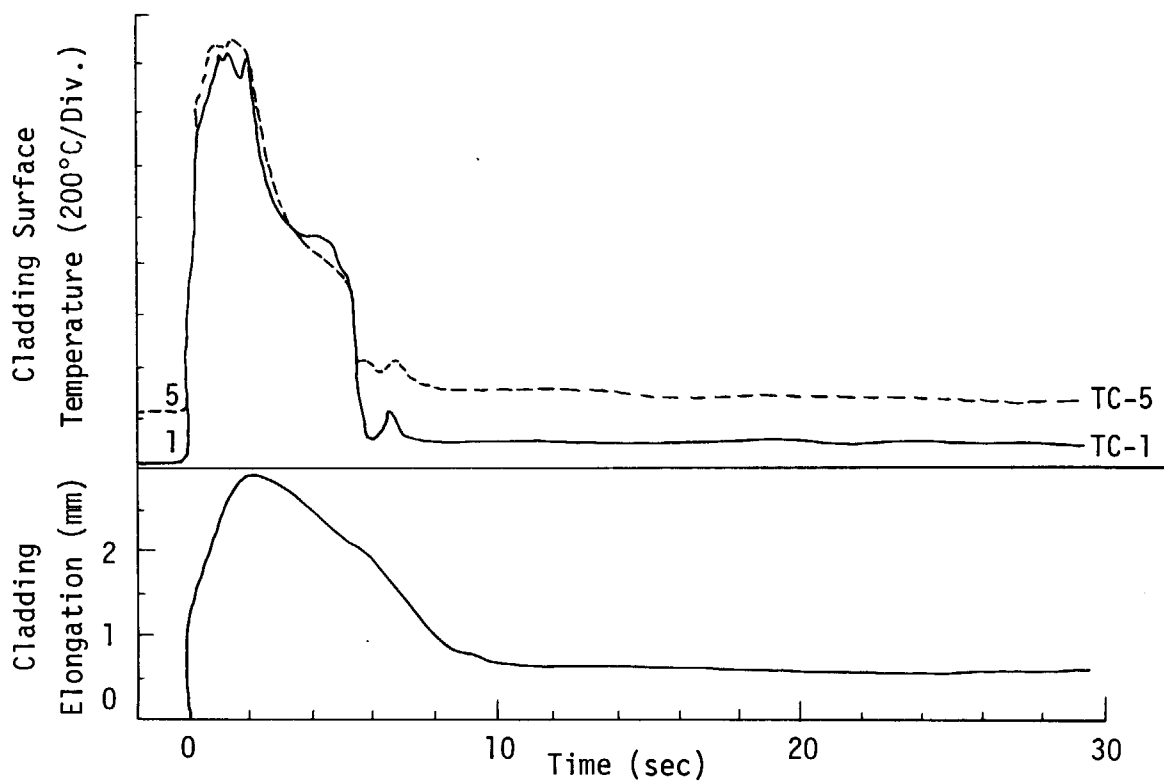
B-17 Transient records of Test No. 502-5 (Zr-lined rod, 394 cal/g.UO₂)



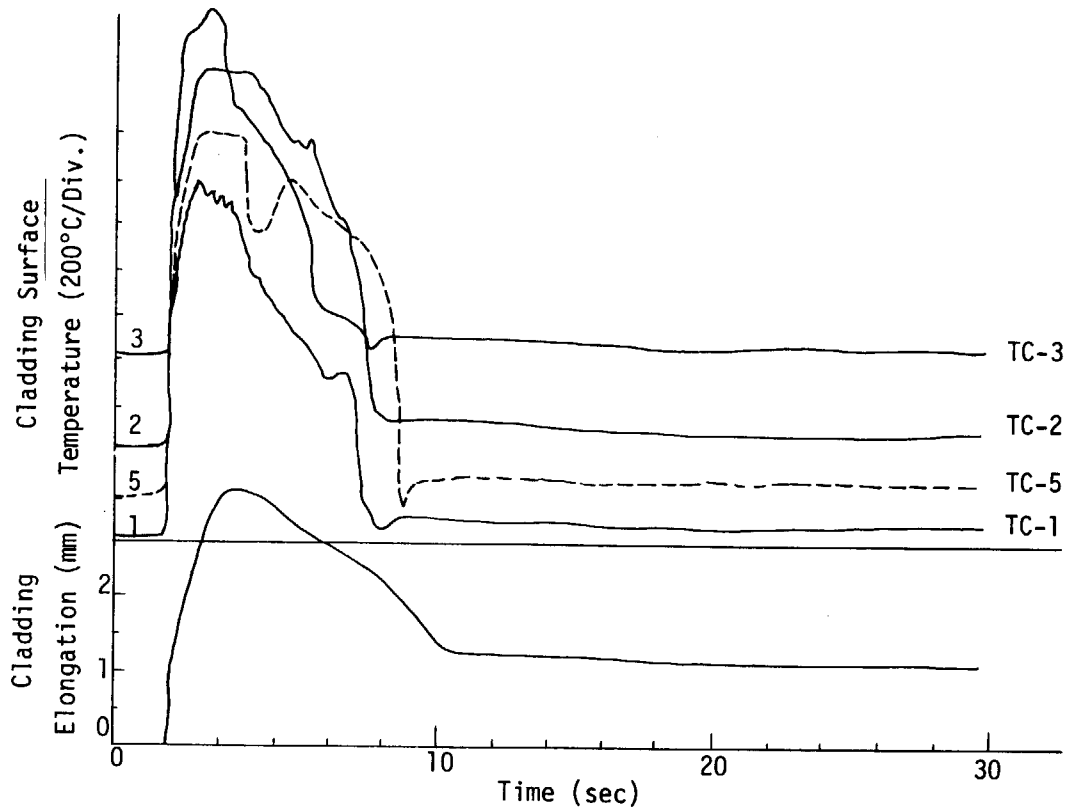
B-18 Transient records of Test No. 503-5 (Cu-barrier rod, 392 cal/g.UO₂)



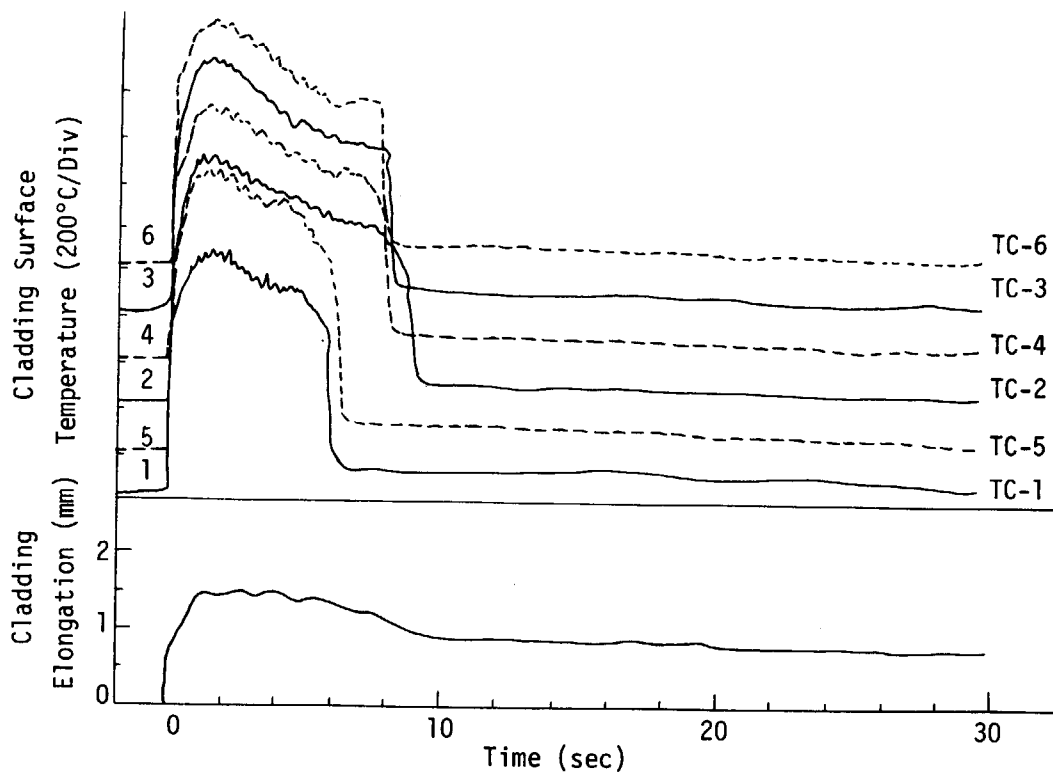
B-19 Transient record of cladding elongation in Test No. 501-2
(Reference rod, 169 cal/g.UO₂)



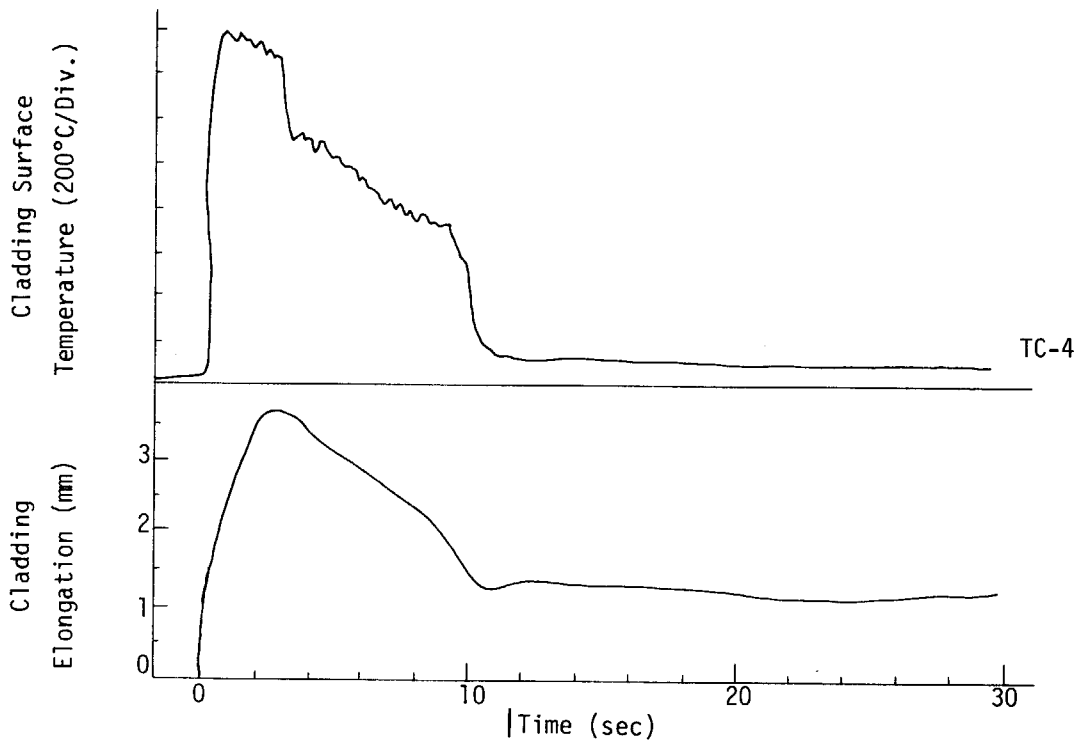
B-20 Transient record of cladding elongation in Test No. 501-4
(Reference rod, 284 cal/g.UO₂)



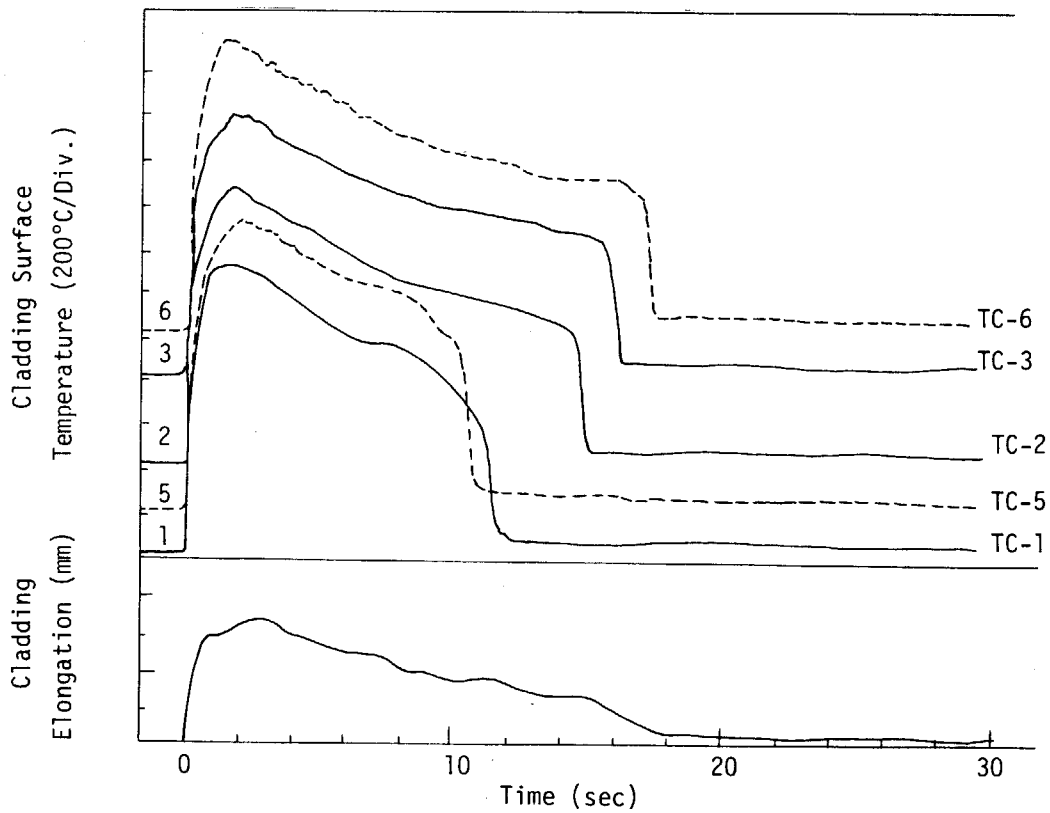
B-21 Transient record of cladding elongation in Test No. 501-7
(Reference rod, 305 cal/g.UO₂)



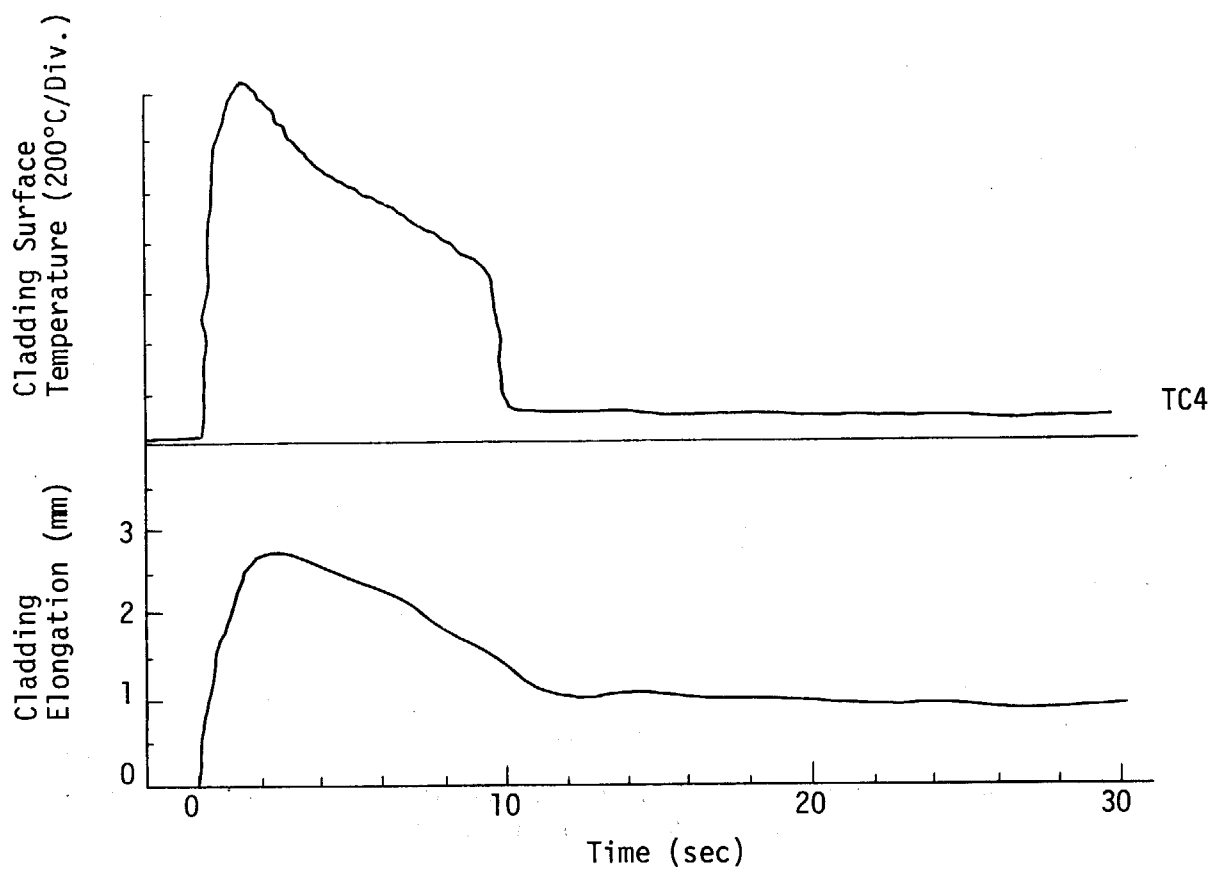
B-22 Transient record of cladding elongation in Test No. 502-1
(Zr-lined rod, 208 cal/g.UO₂)



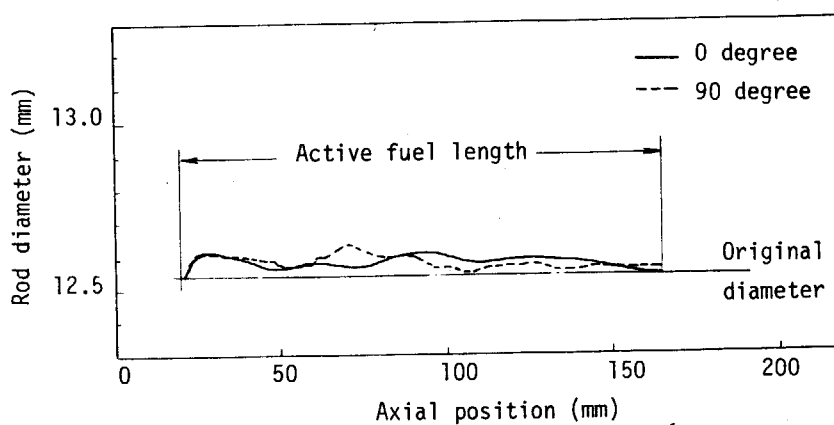
B-23 Transient record of cladding elongation in Test No. 502-3
(Zr-lined rod, 313 cal/g.UO₂)



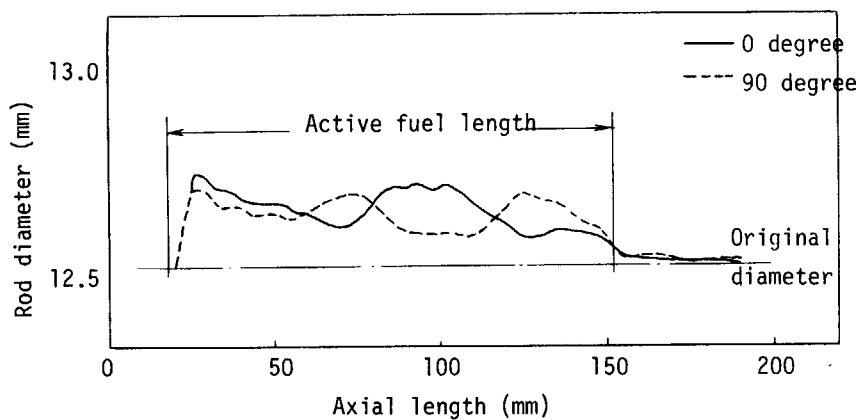
B-24 Transient record of cladding elongation in Test No. 503-1
(Cu-barrier rod, 201 cal/g.UO₂)



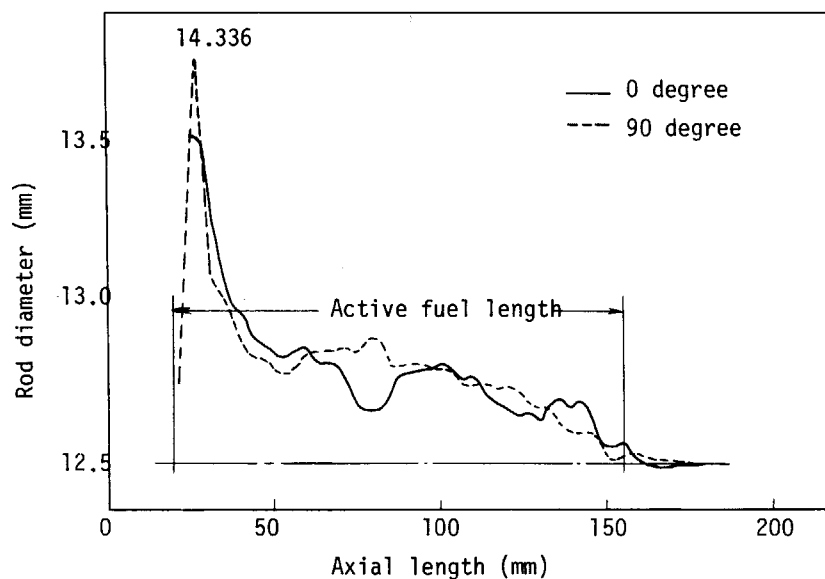
B-25 Transient record of cladding elongation in Test No. 503-3
(Cu-barrier rod, 283 cal/g.UO₂)



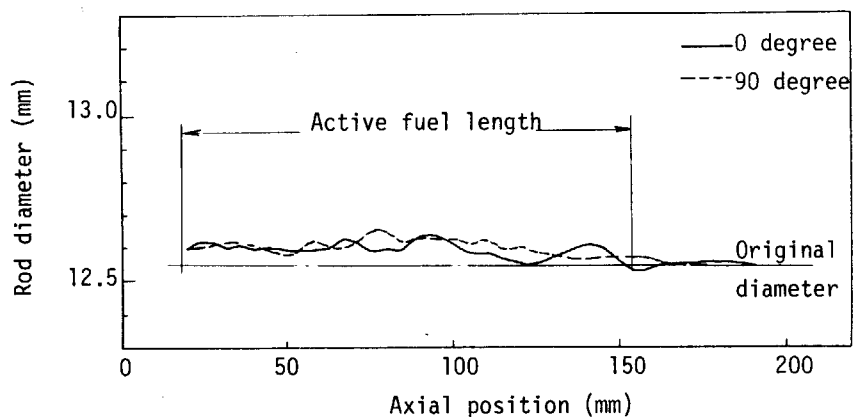
C-1 Diametral profile of a Reference rod in
Test No. 501-1 (209 cal/g.UO₂)



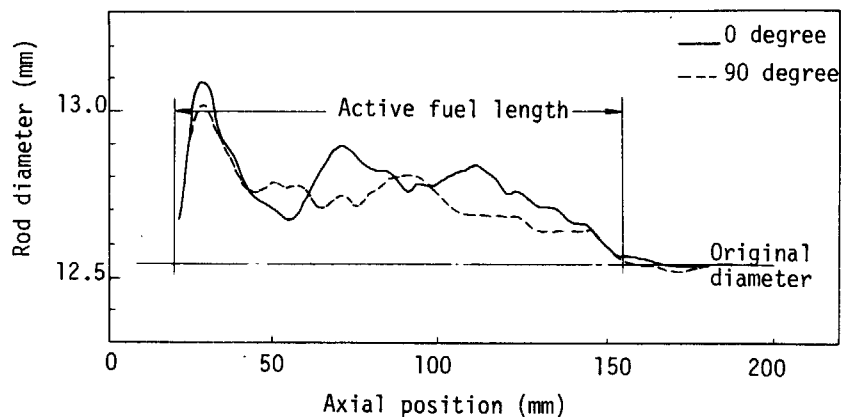
C-2 Diametral profile of a Reference rod in
Test No. 501-3 (257 cal/g.UO₂)



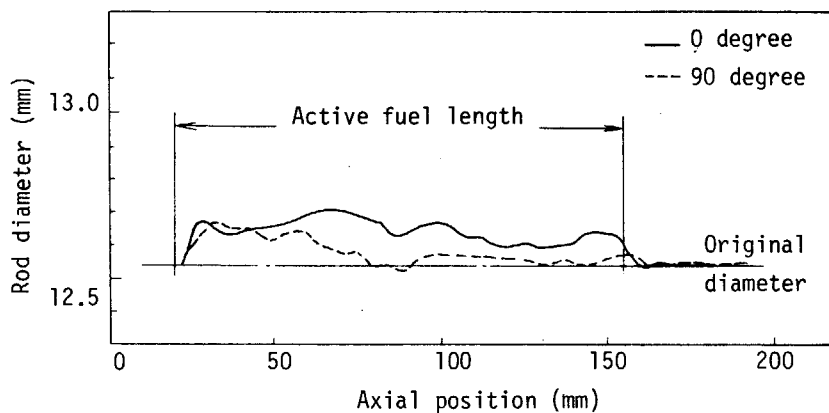
C-3 Diametral profile of a Reference rod in
Test No. 501-4 (284 cal/g.UO₂)



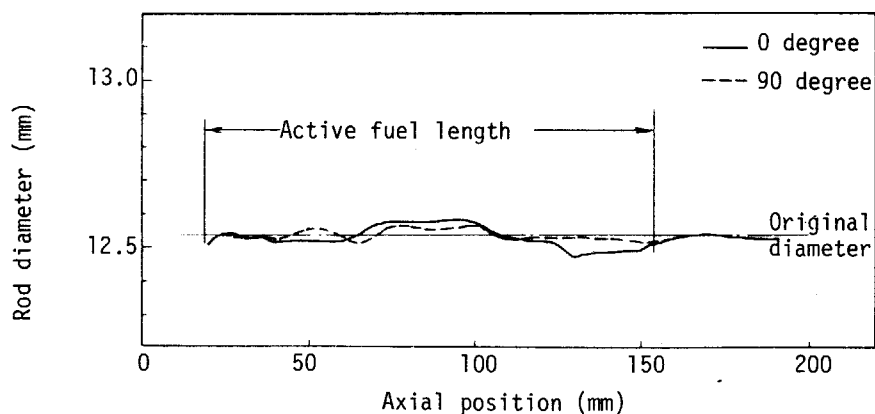
C-4 Diametral profile of a Zr-lined rod in
Test No. 502-1 (208 cal/g.UO₂)



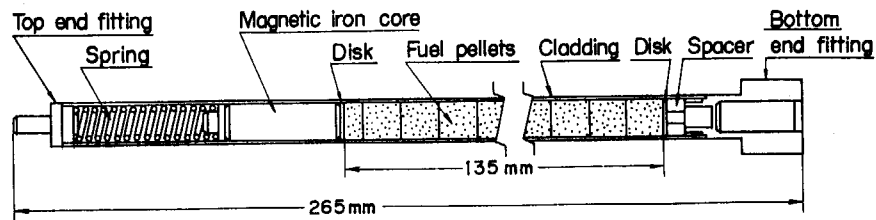
C-5 Diametral profile of a Zr-lined rod in
Test No. 502-4 (304 cal/g.UO₂)



C-6 Diametral profile of a Cu-barrier rod in
Test No. 503-1 (201 cal/g.UO₂)

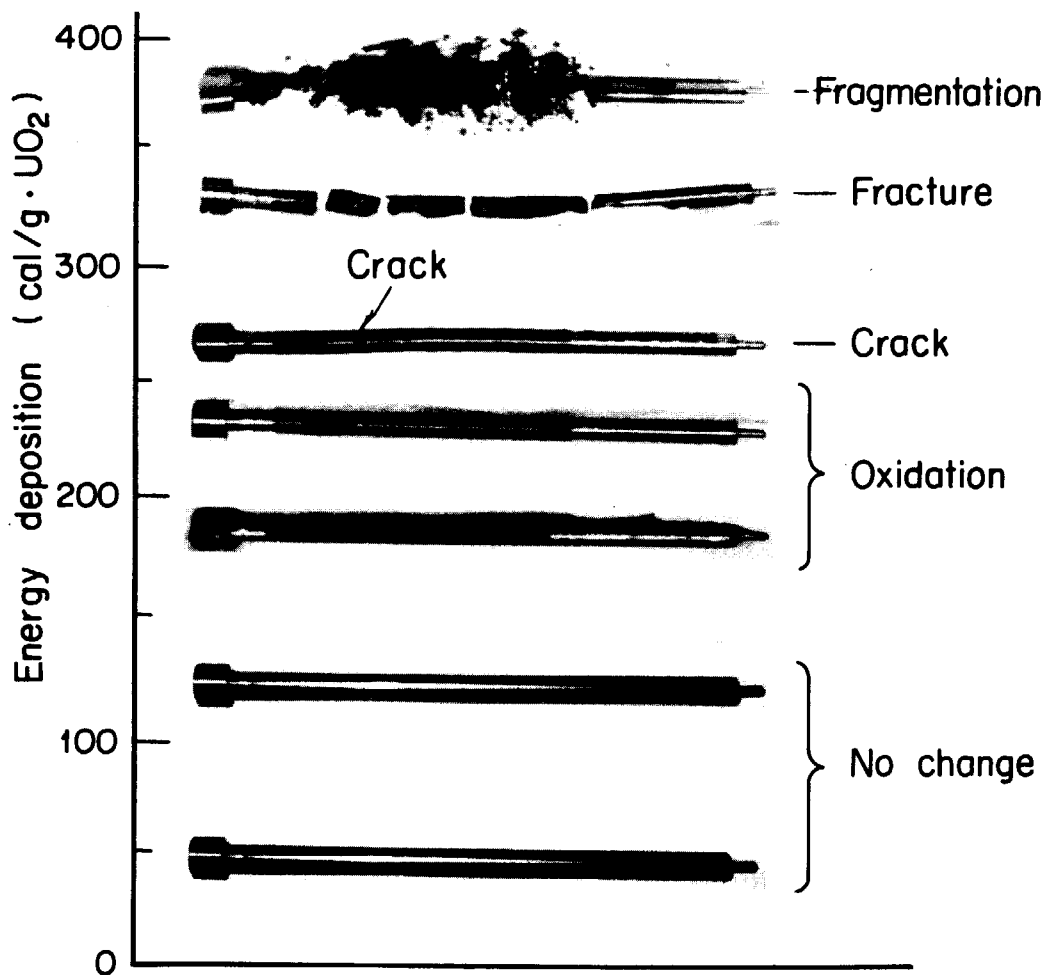


C-7 Diametral profile of a Cu-barrier rod in
Test No. 503-2 (169 cal/g.UO₂)



UO_2 Pellets
 Diameter : 9.29 mm
 Enrichment : 10 %
 Cladding
 Material : Zircaloy-4
 Outer diameter : 10.72 mm
 Wall thickness : 0.62 mm

D-1 NSRR standard test fuel rod



D-2 Appearance of post-test fuel rods in NSRR standard fuel rod tests related with energy deposition